Circuits and Systems Exposition

THE GFT: A GENERAL YET PRACTICAL FEEDBACK THEOREM

R. David Middlebrook

210 Calle Solana, San Dimas, CA 91773

Tel. (909) 592-0317; Fax (909) 592-0698

EMail: rdm@rdmiddlebrook.com

Review Version

Circuits and Systems Exposition

THE GFT: A GENERAL YET PRACTICAL FEEDBACK THEOREM

R. David Middlebrook

Professor Emeritus of Electrical Engineering
California Institute of Technology

ABSTRACT

Feedback systems are usually designed with the familiar single-loop block diagram in mind, that is, the major loop feedback path is designed to have a transmission function such that the specified gain is achieved in the presence of noninfinite major loop gain. Various nonidealities, such as unavoidable minor loops and direct forward transmission, make the single-loop block diagram progressively less useful, especially at higher frequencies.

A general feedback theorem (GFT) enables the major loop to be identified at all frequencies, and gives a unique description of the closed-loop gain in terms of three component transfer functions: the ideal closed-loop gain G_∞, the loop gain T, and the null loop gain T_n. The loop gain and the null loop gain are each composed of a current return ratio, a voltage return ratio, and an interaction term, all of which can easily be calculated under certain null conditions that are established by test signal injection. An alternative form presents the closed-loop gain as a weighted sum of G_∞, the gain with $T = \infty$, and G_0, the gain with $T = 0$.

The GFT defines a "natural" block diagram model that is identical in format to the single-loop model that is conventionally assumed, thus providing a link between general feedback theory and a detailed circuit diagram analyzed in terms of factored pole-zero transfer functions. Different test signal injection points produce different loop gains, and a "principal loop gain" is defined.

The GFT is illustrated on a two-stage feedback amplifier having various nonidealities, including loading interactions at all points, direct forward transmission, and two minor loops.

The GFT is computer friendly. Once the null injection conditions have been programmed, a user unfamiliar with null injection can obtain all the results on any circuit simulator program. The symbolic results for the two-stage amplifier example are verified numerically with use of an Intusoft ICAP/4 simulator.

There are many reviews of the various standard approaches to modeling and analysis of feedback systems, for example [1] and [2]. At one extreme, the "bottom up" approach reviewed in Section 1, an effort is made to preserve the concept of a single loop represented as a block diagram describing a forward path and a feedback path, and the spotlight is on the loop gain. The model can be augmented to account for loading effects and direct forward transmission, but encounters difficulties when internal minor feedback loops are present. At the other extreme, the "top down" approach, the system is treated as a whole, with or without a flowgraph model, and the spotlight is on the return ratios of its various elements; a block diagram is one of the results rather than the starting point.

Modeling a feedback system as a combination of two two-port models seems to combine the worst features of both extreme methods. One of the four possible connections has to be specified at the outset, and three of them (those having a series connection at one or both ends) are incomplete models because of failure to include common-mode signal transmission in the forward path. In the example circuit treated in Section 4, it is found that this common-mode feedforward makes a greater contribution to the direct forward transmission than does the feedforward through the feedback path. In addition, use of two-port models effectively establishes a firewall between the analysis results and the physical operation of the system, which makes the analysis almost useless for design.

The "feedback theorem" developed in this paper represents a "top down" approach that combines the best features of the two extreme approaches, and its greatest benefit is that its constituent transfer functions can be calculated, both symbolically and by simulation, from the circuit diagram and therefore have direct physical interpretations. The theorem is derived on a system basis in Section 2 as a General Network Theorem (GNT) in terms of return ratios without mention of "feedback", but the format is immediately identifiable as describing a single-loop model with direct forward transmission accounted for separately, as in the "natural" block diagram model of Fig. 7. Since this block diagram is identical to that in Fig. 3 or 4 postulated as the starting point of the "bottom up" approach, it is convenient to re-name the GNT as the General Feedback Theorem (GFT), and the corresponding nomenclature is developed in Section 3.

Section 4 treats a two-stage feedback amplifier circuit that contains all the nonidealities that ultimately paralyze the "bottom up" approach. The GFT is used in Section 4.1 to find the voltage gain of the amplifier and, since the GFT applies to any transfer function of a linear system, it is used in Section 4.2 to find the output impedance of the same amplifier. All results are verified numerically by use of a circuit simulator.

Some corollaries and different interpretations and perspectives of the GFT are discussed in Section 5, and conclusions are summarized in Section 6.

1. The "Bottom Up" Approach

A designer/analyst usually designs a feedback system with the familiar single-loop block diagram of Fig. 1 in mind, that is, the major loop feedback path is designed to have a transmission function such that the specified gain is achieved in the presence of noninfinite major loop gain.

Figure 1 is a direct representation of the servomechanism type of application, in which A is variously the "forward gain," the "open-loop gain," or the "gain without feedback," and K is the "feedback divider ratio," or the fraction of the

output that is fed back to the input. The input and output signals u_i, u_o can be any combination of voltage, current, torque, velocity etc. whose ratio is the transfer function of interest, the "closed-loop" gain G given by

$$G \equiv \frac{u_o}{u_i} = \frac{A}{1+AK} \tag{1}$$

As circuit complexity increases, various nonidealities emerge that are not accounted for in the simple model of Fig. 1. A common approach is to augment the model to account for certain nonidealities, make approximations, or, as a last resort, ignore them.

Figure 1, and the corresponding format (1), suggest that the A and K blocks should be designed separately so that the resulting closed-loop gain G meets some specification. The trouble begins right here, because the two blocks in many cases are not really separable. That is, the feedback path loads the forward path at both input and output, so that breaking the loop at either point upsets the loading and gives wrong answers for A and/or K. Attempts may be made to convince oneself that a loading is negligible or, if not, to invoke a dummy load to simulate a disconnected block.

An alternative is to eliminate the need to calculate A separately, by a simple rearrangement of (1):

$$G \equiv \frac{1}{K}\frac{AK}{1+AK} = G_\infty \frac{T}{1+T} = G_\infty D \tag{2}$$

where

$$G_\infty \equiv \frac{1}{K} \tag{3},$$

$$T \equiv AK \tag{4}$$

$$D \equiv \frac{T}{1+T} \tag{5}$$

The loop no longer need be broken at the input or output of the A block, but can be broken at some other point where the loading is absent. Such a point is likely to be found inside the forward path wherein reside the active devices whose outputs can be modeled, at least approximately, by controlled generators. The loop gain T can be found by applying a test signal at the new break point, and observing the signal that returns around the loop to the other side of the break.

However, it is preferable, for several reasons, not to break the loop but to inject a test signal u_z into the closed-loop at that same point, as shown in Fig. 2. The u's can be all voltages or all currents. The choice is not arbitrary: they must be currents if the output of the A_1 block is a controlled current generator, voltages if the output is a controlled voltage generator. In either case, the loop gain T is u_y / u_x with $u_i = 0$.

There is another benefit in rearranging (1) into (2). The result for the closed-loop gain G is expressed in terms of two transfer functions G_∞ and T, each of which has individual significance: G_∞ is the limiting value of G when the loop gain T becomes infinite, and so can be interpreted as the "ideal closed-loop gain;" how large T is determines how close the actual G is to G_∞, by way of the "discrepancy factor" $D \equiv T/(1+T)$.

Whereas T is a single-injection transfer function, in that u_z is the only independent source present for its calculation, G_∞ is a null double-injection transfer function made under the condition of simulated infinite T. With reference to Fig. 2,

u_z is assumed adjusted relative to u_i so that u_y is nulled, which propagates back as a nulled error signal at the feedback summing point. Thus, the output is driven by u_z to a value such that the fedback signal exactly matches the input signal with zero error, so that G_∞ is u_o / u_i with u_y nulled.

The overall design of a feedback system can be laid out in three steps:

Design Step #1. Design the feedback network so that G_∞ meets the specification;

Design Step #2. Design the loop gain so that T is large enough that the actual G meets the specification within the allowed tolerances;

Design Step #3. Since in any real system T drops below unity beyond some "crossover" frequency, design T to be large enough up to a sufficiently high frequency. In an ac coupled system, a dual condition occurs in the reverse frequency direction. Usually, #3 is the only difficult step.

Although not explicitly stated, Design Step #3 includes the stability requirement. The discrepancy factor $D \approx 1$ when $T >> 1$, and $D \approx T$ when $T << 1$; the transition between these two ranges, which is not necessarily a monotonic decrease, occurs at the loop gain crossover frequency w_c, the frequency at which $| T | = 1$. If the phase margin of T is less than about 60°, D begins to peak up in the neighborhood of the crossover frequency, and in the limit of zero phase margin the peak in D becomes infinite, which marks the onset of instability. Thus, the discrepancy factor D must not be allowed to peak up beyond the tolerance limit of the specification, which is a much more stringent design requirement than mere "stability".

While shifting the u_z test signal injection point to a controlled generator alleviates the loading problem between the A and K blocks in Fig. 1, another nonideality requires an augmentation of the model. The use of arrowheads rather than rectangles to represent the blocks in Figs. 1 and 2 specifically implies that the signal travels in only one direction. This may be a good approximation for the forward path, but is usually not a good approximation for the feedback path, which is normally a passive network having comparable transmissions in the two directions.

This nonideality can be accommodated by addition of another block G_0 as in Fig. 3. By the basic single-loop properties, an interference signal injected into the loop contributes an additive term to the output equal to the interference divided by the feedback factor $1+T$, so by identifying the interference as the input signal u_i injected through the G_0 block, (2) is augmented as follows:

$$G = G_\infty \frac{T}{1+T} + G_0 \frac{1}{1+T} \qquad (6)$$

The "direct forward transmission" block G_0 can be evaluated as another null double injection transfer function of the model of Fig. 3. This time zero, instead of infinite, loop gain T is simulated by adjustment of u_z relative to u_i such that u_x is nulled; that is, u_z soaks up u_y leaving no drive to the output. Hence, any output u_o that appears must have come through the G_0 block, and G_0 is u_o / u_i with u_x nulled.

The "augmented feedback theorem" of (6) indicates that the closed-loop gain G can be considered as the weighted sum of the gain G_∞ with T infinite and the gain G_0 with T zero. The G_∞ contribution dominates when the loop gain T is large (below loop-gain crossover), and the G_0 contribution dominates when T is small (beyond crossover).

There is another version of (6), in terms of a fourth transfer function, identified as the "null loop gain" T_n, that replaces G_0:

$$G = G_\infty \frac{1+\frac{1}{T_n}}{1+\frac{1}{T}} \tag{7}$$

where

$$\frac{T_n}{T} \equiv \frac{G_\infty}{G_0} \tag{8}$$

The null loop gain T_n can be evaluated as another null double injection transfer function of the model of Fig. 3 , namely u_y / u_x with u_o nulled. The physical interpretation of this condition is that u_z is adjusted relative to u_i such that u_x drives the output to a value equal to and opposite from the value driven through the G_0 block; hence the reciprocal relationship expressed by (8).

The presence of the augmented term $(1+1/T_n)$ in (7) adds Step #4 to the procedure for design of a feedback system:

Design Step #4. Design the null loop gain so that T_n is large enough that the actual G meets the specification within the allowed tolerances.

Even though the physical interpretation of T_n may be less obvious than that of G_0, its use may be preferable for two reasons. First, to determine the relative importance of the augmented term in (7), T_n need merely be compared to unity; to determine the relative importance of the augmented term in (6), G_0 has to be compared with $G_\infty T$. Second, direct determination of T_n by the null double injection condition is usually shorter and easier than that of G_0.

The above short discussion summarizes detailed treatments in [3] — [5], the objective of which is to retain the single-loop model of Fig. 1 despite complications caused by various nonidealities. There are still hidden limitations, however. Test signal u_z injection must be at an ideal controlled generator, defined as an "ideal injection point": if at a controlled current generator, the loop gain T and the null loop gain T_n are evaluated as current return ratios; if at a controlled voltage generator, they are evaluated as voltage return ratios.

Unfortunately, in real electronic systems ideal controlled generators do not exist. Controlled generators occur in the outputs of models of active devices, but there is always a nonzero admittance connecting the generator output back to its controlling input. While this admittance may be negligible at low frequencies, its capacitive component, representing the drain-gate capacitance of an FET or the collector-base capacitance of a BJT, always ultimately shorts out the generator at sufficiently high frequencies.

Consequently, calculation of the u_y / u_x ratio does not give the "right" answers for the loop gain and the null loop gain, and the results usually break down in the frequency range surrounding loop gain crossover, just where accurate results are needed to evaluate phase margin.

The last nonideality needed to be accommodated are these nonzero admittances, which constitute in general local, or minor, feedback loops within the major loop, as shown in Fig. 4. Although an effort was made in [4] to extend the calculation of the loop gain T to allow for a nonideal injection point, the result was not complete.

It is the purpose of this paper to overcome this remaining limitation, and to provide a general feedback theorem that gives exact answers for the general model of Fig. 4. Interestingly, the two formats of (6) and (7) still apply; the principal differences are that the four transfer functions G_∞, T, T_n, and G_0 require extended definitions, and the last three each consists of the sum of three terms.

2. A "Top Down" Approach: The General Network Theorem (GNT)

The evolution of the model as described by Figs. 1 through 4 indicates that several nonidealities were accommodated by patching up the original simple model. In contrast, the development of the General Network Theorem (GNT) begins with a clean slate, simply the single block of Fig. 5(a), in which arbitrary nodes W and XY are identified. The only constraint on the content of the block is that it is a linear circuit model. The output u_o and input u_i designate any transfer function of interest, $H = u_o / u_i$, where H replaces G to preclude any implication that the transfer function is limited to a "gain."

The following steps are to be executed:

Analysis Step 1. In Fig. 5(a), separate node XY into two nodes and insert between nodes X, Y, and W an ideal transformer, represented by a controlled current generator and a controlled voltage generator, together with identified voltages and currents as shown in Fig. 5(b). "Normal" values of the controlled generators are $A_i = 1$, $A_v = 1$ so that the ideal transformer is transparent and its presence does not affect the normal system transfer function H.

Analysis Step 2. Designate reference values of the two controlled generators as $A_i = 0$, $A_v = 0$, which causes H to change to a reference value H_{ref}. From Fig. 5(b), zero values of the controlled generators are equivalent to both i_y and v_y being nulled. Thus,

$$H_{ref} \equiv \left.\frac{u_o}{u_i}\right|_{\substack{A_i=0\\A_v=0}} = \left.\frac{u_o}{u_i}\right|_{\substack{i_y=0\\v_y=0}} \equiv H^{i_y v_y} \tag{9}$$

where, to simplify the notation, a signal that is nulled is shown as a superscript upon the quantity being calculated.

Analysis Step 3. Reinstate the controlled generators A_i and A_v via the Extra Element Theorem, and set them equal to unity.

Null double injection, the Extra Element Theorem (EET), the Two Extra Element Theorem (2EET), and the N Extra Element Theorem (NEET) are extensively discussed in [6] — [9].

The theorem correction factor has a numerator and a denominator, each of which has the same form. If an "extra element" is an impedance Z, each contains the ratio of Z to a certain driving point impedance seen by Z. If the extra element is a controlled generator, such as A_i in Fig. 5(b), the denominator contains the ratio of A_i to the negative of a return ratio seen by A_i, evaluated with the input u_i set to zero; the numerator contains the ratio A_i to the negative of a return ratio seen by A_i evaluated with the output u_o nulled.

The controlled generators A_v and A_i can be reinstated sequentially with use of the (single) EET. If A_v is reinstated first,

$$H^{i_y} = H^{i_y v_y} \frac{1+\dfrac{A_v}{T_{nv}^{i_y}}}{1+\dfrac{A_v}{T_v^{i_y}}} \tag{10}$$

The notation is that T_v represents a voltage return ratio, and subscript n indicates that the ratio is calculated with the output u_o nulled, rather than with the input u_i set to zero. The superscript i_y indicates that all four parameters are evaluated with i_y nulled because A_i is still at its reference value zero.

The controlled generator A_i can now be reinstated by a second application of the EET correction factor to the reference value H^{i_y}:

$$H = H^{i_y} \frac{1+\dfrac{A_i}{T_{ni}}}{1+\dfrac{A_i}{T_i}} \tag{11}$$

in which T_i represents a current return ratio. Since T_i is to be evaluated with A_v already reinstated, it can be expressed in terms of its value $T_i^{v_y}$ with A_v=0 by a "nested" application of the EET:

$$T_i = T_i^{v_y} \frac{1+\dfrac{A_v}{T_v^{i_y}}}{1+\dfrac{A_v}{T_v^{i_x}}} \tag{12}$$

in which $T_v^{i_x}$ is the return ratio for A_v with the "input" i_x of the transfer function T_i set to zero, and $T_v^{i_y}$ is the return ratio for A_v with the "output" i_y of the transfer function T_i nulled.

In the same way, T_{ni} in (11) can be expressed in terms of its value $T_{ni}^{v_y}$:

$$T_{ni} = T_{ni}^{v_y} \frac{1+\dfrac{A_v}{T_{nv}^{i_y}}}{1+\dfrac{A_v}{T_{nv}^{i_x}}} \tag{13}$$

Equations (10), (12), and (13) can be substituted into (11) to give

$$H = H^{i_y v_y} \frac{1+\dfrac{A_i}{T_{ni}^{v_y}}+\dfrac{A_v}{T_{nv}^{i_y}}+\dfrac{A_i A_v}{T_{ni}^{v_y} T_{nv}^{i_x}}}{1+\dfrac{A_i}{T_i^{v_y}}+\dfrac{A_v}{T_v^{i_y}}+\dfrac{A_i A_v}{T_i^{v_y} T_v^{i_x}}} \tag{14}$$

which is the result for H in terms solely of parameters evaluated for both A_i and A_v zero, and could have been obtained directly from the 2EET.

The above derivation could have been done with A_i reinstated before A_v, in which case dual versions of (10) through (14) would have been obtained. Since these dual versions of (14) must be the same , it follows that the dual versions of the two

product terms in (14) must be equal, which allows dual definitions of the product terms:

$$T_{iv} \equiv T_i^{v_x} T_v^{i_y} = T_i^{v_y} T_v^{i_x} \tag{15}$$

$$T_{niv} \equiv T_{ni}^{v_x} T_{nv}^{i_y} = T_{ni}^{v_y} T_{nv}^{i_x} \tag{16}$$

It remains only to restore the controlled generators to their normal values $A_i = 1$, $A_v = 1$ to give

$$H = H^{i_y v_y} \frac{1 + \dfrac{1}{T_{ni}^{v_y}} + \dfrac{1}{T_{nv}^{i_y}} + \dfrac{1}{T_{niv}}}{1 + \dfrac{1}{T_i^{v_y}} + \dfrac{1}{T_v^{i_y}} + \dfrac{1}{T_{iv}}} \tag{17}$$

This result for the "first-level" transfer function H can be written

$$H = H_\infty \frac{1 + \dfrac{1}{T_n}}{1 + \dfrac{1}{T}} \tag{18}$$

which is in the same format as (7), but with altered and extended definitions of the component "second-level" transfer functions H_∞, T, and T_n:

$$H_\infty \equiv H^{i_y v_y} \tag{19}$$

$$\frac{1}{T} \equiv \frac{1}{T_i^{v_y}} + \frac{1}{T_v^{i_y}} + \frac{1}{T_{iv}} \tag{20}$$

$$\frac{1}{T_n} \equiv \frac{1}{T_{ni}^{v_y}} + \frac{1}{T_{nv}^{i_y}} + \frac{1}{T_{niv}} \tag{21}$$

Equation (18), together with the extended definitions of (19) through (21), may be designated as a General Network Theorem (GNT), since it applies to any network subject only to the constraint of linearity.

All the parameters of the GNT in (15) through (17), designated "third-level" transfer functions, can be evaluated by appropriate adjustment of the input signal u_i and two test signals j_z and e_z injected in place of the ideal transformer of Fig. 5(b), as shown in Fig. 6. For example, $H^{i_y v_y}$ is given by (9). The listing of the return ratios is:

j_z and e_z injected:

$$T_i^{v_y} = \left.\frac{i_y}{i_x}\right|_{\substack{v_y=0 \\ u_i=0}} \tag{22}$$

$$T_i^{v_x} = \left.\frac{i_y}{i_x}\right|_{\substack{v_x=0 \\ u_i=0}} \tag{23}$$

$$T_{ni}^{v_y} = \left.\frac{i_y}{i_x}\right|_{\substack{v_y=0 \\ u_o=0}} \tag{24}$$

$$T_{ni}^{v_x} = \left.\frac{i_y}{i_x}\right|_{\substack{v_x=0 \\ u_o=0}} \tag{25}$$

$$T_v^{i_y} = \left.\frac{v_y}{v_x}\right|_{\substack{i_y=0 \\ u_i=0}} \tag{26}$$

$$T_v^{i_x} = \left.\frac{v_y}{v_x}\right|_{\substack{i_x=0 \\ u_i=0}} \tag{27}$$

$$T_{nv}^{i_y} = \left.\frac{v_y}{v_x}\right|_{\substack{i_y=0 \\ u_o=0}} \tag{28}$$

$$T_{nv}^{i_x} = \left.\frac{v_y}{v_x}\right|_{\substack{i_x=0 \\ u_o=0}} \tag{29}$$

The normal value $A_i = 1$ may also be substituted into (11) to give

$$H = H^{i_y}\,\frac{1+\dfrac{1}{T_{ni}}}{1+\dfrac{1}{T_i}} \qquad (30)$$

$$H = H^{v_y}\,\frac{1+\dfrac{1}{T_{nv}}}{1+\dfrac{1}{T_v}} \qquad (34)$$

where

$$H^{i_y} = H^{i_y v_y}\,\frac{1+\dfrac{1}{T_{nv}^{i_y}}}{1+\dfrac{1}{T_v^{i_y}}} \qquad (31)$$

$$H^{v_y} = H^{i_y v_y}\,\frac{1+\dfrac{1}{T_{ni}^{v_y}}}{1+\dfrac{1}{T_i^{v_y}}} \qquad (35)$$

$$T_i = T_i^{v_y}\,\frac{1+\dfrac{1}{T_v^{i_y}}}{1+\dfrac{1}{T_v^{i_x}}} \qquad (32)$$

$$T_v = T_v^{i_y}\,\frac{1+\dfrac{1}{T_i^{v_y}}}{1+\dfrac{1}{T_i^{v_x}}} \qquad (36)$$

$$T_{ni} = T_{ni}^{v_y}\,\frac{1+\dfrac{1}{T_{nv}^{i_y}}}{1+\dfrac{1}{T_{nv}^{i_x}}} \qquad (33)$$

$$T_{nv} = T_{nv}^{i_y}\,\frac{1+\dfrac{1}{T_{ni}^{v_y}}}{1+\dfrac{1}{T_{ni}^{v_x}}} \qquad (37)$$

However, (31) to (33) and (35) to (37) are not needed, because the second level transfer functions in (30) and (34) can be found directly by injection of only one test signal:

j_z injected:

$$H^{i_y} = \left.\frac{u_o}{u_i}\right|_{i_y=0} \qquad (38)$$

$$T_i = \left.\frac{i_y}{i_x}\right|_{u_i=0} \qquad (39)$$

$$T_{ni} = \left.\frac{i_y}{i_x}\right|_{u_o=0} \qquad (40)$$

e_z injected:

$$H^{v_y} = \left.\frac{u_o}{u_i}\right|_{v_y=0} \qquad (41)$$

$$T_v = \left.\frac{v_y}{v_x}\right|_{u_i=0} \qquad (42)$$

$$T_{nv} = \left.\frac{v_y}{v_x}\right|_{u_o=0} \qquad (43)$$

Equations (30) and (34) for a single injected test signal are also in the same format as (18), but with different definitions of the component second-level transfer functions H_∞, T, and T_n than for the dual test signal injection case of (19) through (21).

The above results for the GNT require some interpretation and comment.

Any transfer function of a linear network can be dissected into two successive component levels. Equation (18) shows that the first-level H can be expressed as a combination of a reference transfer function H_∞ and two other transfer functions T and T_n that can provisionally be called respectively the "total return ratio" and the "total null return ratio", all three of which are second-level transfer functions evaluated pursuant to selection of an arbitrary current and/or voltage test signal injection point.

Equations (20) and (21) show that the second-level total return ratios can each be considered as the "triple parallel combination" of a current ratio, a voltage ratio, and a product term defined by (15) and (16), all of which are third-level quantities.

The symmetry between the entire expressions (20) and (21) for T and T_n may also be noted: all the return ratios comprising T are evaluated with the input signal u_i set to zero; all those comprising T_n are evaluated with the output u_o nulled.

Most important, with respect to the third-level transfer functions (9), and (22) through (29), is that all of them are to be evaluated with at least one quantity nulled. Null injection, discussed in detail in [6], is a concept whose usefulness and simplicity may not be familiar, and so the meaning and significance will be reviewed here.

The four T's of (22), (23) and (26), (27) all demand null double injection calculations upon the model of Fig. 6. Since all four are for $u_i = 0$, j_z and e_z are the two injected signals. Since the model is linear, any signal in the system is the linear sum of separate contributions from j_z and e_z, and a unique ratio exists between j_z and e_z which causes any selected dependent signal in the system to be nulled. Since all other signals are also the linear sum of contributions from the two injected test signals, the unique ratio that nulls a selected signal can be invoked to find the ratio of any two other signals. In principle, this procedure can be employed to calculate the four T's.

In practice, however, it is not necessary to evaluate the unique ratio in order insert it in the two contributions to any other signal. Instead, the mere existence of the null constitutes equivalent information that can be used directly to evaluate any signal in terms of another. For example, to calculate $T_i^{v_y}$ for the hidden circuit of Fig. 6, start with i_x and multiply it by successive factors as the signal progresses through the circuit, making use of the nulled v_y (and the zero u_i) where necessary along the way. Eventually the signal shows up as i_y in the form of a multiple of i_x, and this multiple is the desired $T_i^{v_y}$. Note that the value of neither test signal, nor their ratio, has been needed in this process.

This "short cut" is the key to the simplicity and ease of use of null double injection. It is no accident that a null double injection calculation is simpler and easier than the same calculation under single injection: the null "propagates", so that if one signal is null, other signals may also be nulled; any circuit element that supports a nulled voltage or current is absent from the final result.

A logical extension suggests that if three independent signals are present, two other signals can be nulled and the double-null triple injection calculation should be even simpler and easier, which is in fact the case. The four T_n's and the reference transfer function $H^{i_y v_y}$ all demand double-null triple injection conditions. The input u_i and the injected test signals j_z and v_z are all present, and for $H^{i_y v_y}$, for example, i_y and v_y are to be nulled. Again the short-cut is to start with u_i and multiply it by successive factors as the signal progresses through the circuit, making use of the nulled i_y and v_y where necessary along the way. Eventually the signal shows up as u_o in the form of a multiple of u_i, and this multiple is the desired $H^{i_y v_y}$.

Since the GNT (18) has the same form as (7), it also can be expressed in the form corresponding to (6):

$$H = H_\infty \frac{T}{1+T} + H_0 \frac{1}{1+T} \tag{44}$$

where H_0 is an alternative second-level transfer function related to T_n by the "redundancy relation"

$$\frac{H_0}{H_\infty} = \frac{T}{T_n} \tag{45}$$

Since $1/T_n$ has three components, H_0 can likewise be expressed as the sum of three components. However, for some first-level transfer functions, $H_\infty = 0$ and $T_n = 0$ so H_0 cannot be found from (45). Instead, the three components of H_0 can be evaluated independently in terms of three third-level calculations upon the model of Fig. 6, as follows.

As discussed in [7], there are four versions of the 2EET, corresponding to the four combinations of reference values of the two extra elements, either of which may be chosen as zero or infinite. Likewise, there are three other versions of (17), corresponding to the three other combinations of reference values of A_i and A_v. The combination chosen for (17) is reference values $A_i = 0$, $A_v = 0$, which is equivalent to $i_y = 0$, $v_y = 0$, for which the reference value of H is $H^{i_y v_y}$. The other three reference values of H can be found by extraction of one term in the numerator and the corresponding term in the denominator from (17), and combining these two terms with $H^{i_y v_y}$:

$$H^{v_y i_x} = \frac{T_i^{v_y}}{T_{ni}^{v_y}} H^{i_y v_y} \tag{46}$$

$$H^{i_y v_x} = \frac{T_v^{i_y}}{T_{nv}^{i_y}} H^{i_y v_y} \tag{47}$$

$$H^{i_x v_x} = \frac{T_{iv}}{T_{niv}} H^{i_y v_y} \tag{48}$$

The correction factor belonging to each reference value of H also emerges from this process, but these are not needed here.

Finally, substitution into (45) of the three components of $1/T_n$ from (21) and replacement of H_∞ from (46) through (48) leads to

$$H_0 = H^{v_y i_x} \frac{T}{T_i^{v_y}} + H^{i_y v_x} \frac{T}{T_v^{i_y}} + H^{i_x v_x} \frac{T}{T_{iv}} \tag{49}$$

The three reference values of H defined by (46) through (48) are all double-null triple injection transfer functions defined similarly to $H^{i_y v_y}$ in (9):

$$H^{v_y i_x} \equiv \left.\frac{u_o}{u_i}\right|_{\substack{v_y=0 \\ i_x=0}} \quad (50) \qquad H^{i_y v_x} \equiv \left.\frac{u_o}{u_i}\right|_{\substack{i_y=0 \\ v_x=0}} \quad (51) \qquad H^{i_x v_x} \equiv \left.\frac{u_o}{u_i}\right|_{\substack{i_x=0 \\ v_x=0}} \quad (52)$$

For the single EET, there are only two versions corresponding to the two combinations of reference values of the extra element. In (30) the reference value is A_i=0, which defines H^{i_y}. By extraction of T_{ni} from the numerator and T_i from the denominator of (30), the other reference value H^{i_x} for A_i=∞ is

$$H^{i_x} = \frac{T_i}{T_{ni}} H^{i_y} \tag{53}$$

where

$$H^{i_x} = \left.\frac{u_o}{u_i}\right|_{i_x=0} \tag{54}$$

This is the redundancy relation (45) for the single EET, and so for single current injection

$$H_0 = H^{i_x} \tag{55}$$

A similar treatment for (34), the single EET for the extra element A_v, leads to

$$H^{v_x} = \frac{T_v}{T_{nv}} H^{v_y} \tag{56}$$

where

$$H^{v_x} = \left.\frac{u_o}{u_i}\right|_{v_x=0} \tag{57}$$

and so for single voltage injection

$$H_0 = H^{v_x} \tag{58}$$

Thus, according to whether dual or single test signal injection is employed, H_0 in (44) can be found from (49), (55), or (58). Each reference value of H in H_0 is a third-level transfer function, and may be calculated from Fig. 6 by the "short-cut" method.

In summary, injection of a test current and/or a test voltage at an arbitrary point in a linear circuit model as in Fig. 6 permits calculation of a number of single injection, null double injection, and double null triple injection transfer functions. These third-level quantities can be assembled to give the second-level transfer functions H_∞, T, T_n, H_0 which in turn can be combined in (18)or (44) to give the desired result, an overall first-level transfer function H in the absence of the injected test signals.

This "divide and conquer" approach has several advantages over the conventional direct calculation of H. Most important, the single high entropy expression for H is replaced by several other expressions that can more readily be derived in low entropy form. A low entropy expression [10] is one in which element symbols are grouped so as to reveal their origin in the circuit model, and also so that their relative contribution to the result is exposed by substitution of numerical values. For example, impedances are grouped as ratios and series-parallel combinations. The short-cut method of calculating the third-level null injection transfer functions is well-suited to build low-entropy expressions directly. Because the total return ratio T and the total null return ratio T_n are each parallel combinations of the third-level quantities, the low entropy format is retained in the second-level transfer functions T and T_n.

The greatest advantage is that substitution of the second-level quantities into the general theorem (18) or (44) need not actually be carried out: there is no benefit in throwing away the extra useful information contained in low entropy expressions by multiplying out (18) or (44) into an amorphous ratio of sums of products of the element values. For design-oriented analysis, the useful information is contained in H_∞, T, T_n, H_0: these are the functions that have to be "designed", according to Design Steps #1 through #4 described above.

It should be emphasized that the GNT of (18) or (44) is completely general; the only constraint is that it applies to a linear system model. The transfer function H can be a voltage gain, current gain, transimmittance, or self-immittance.

An aspect of the generality is that any injection point can be chosen for the test current and voltage. Different sets of second-level transfer functions H_∞, T, T_n, H_0 result from different injection points, although if any of these sets is inserted into the general theorem, the same result for H is of course obtained. As mentioned above, this insertion is not needed, because H_∞, T, T_n, H_0 are themselves the design-oriented results that are of interest.

The format of the GNT exposes the total return ratio T and the total null return ratio T_n of a fictitious ideal transformer inserted at an arbitrary point in the circuit, in which each is a parallel combination of a current return ratio of the transformer controlled current generator, a voltage return ratio of the transformer controlled voltage generator, and an interaction term according to (15) and (16). The format arises as a form of the EET in which the two transformer controlled generators are identified as "extra elements." As already seen, only one such transformer controlled generator need be so identified, which leads to a format in which T and T_n represent only a single current or a single voltage return ratio, as appropriate.

This procedure can be extended in principle to any number of inserted ideal transformers, which results in a GNT derived from the NEET in terms of total return ratios having additional contributing return ratios. Two such transformers might give a GNT useful in describing a circuit having both differential and common-mode feedback loops. A special case of the two-transformer model identifies the current return ratio of one transformer and the voltage return ratio of the other as the two extra elements, which means that the GNT of (18) or (44) is unaltered even if separate injection points are used for the test signals j_z and e_z. Another special case identifies either the two controlled current generators or the two controlled voltage generators as extra elements, meaning that two test currents or two test voltages could be injected at different points in the circuit. The GNT of (18) or (44) would still be unaltered, except that the subscript notation would have to be changed from i and v to i_1 and i_2 or v_1 and v_2.

More than one fictitious ideal transformer will not be further considered in this paper, and the discussion will be limited to the test signal injection model of Fig. 5(b), including the special cases in which one of the test signals is zero. The three currents i_x, i_y, j_z, and the three voltages v_x v_y, e_z each form a phasor triangle.

The term "injection point" needs to be more specifically defined. Actually, since the calculations are to be done only with respect to the injected test signals j_z and/or e_z, what is needed is an identification of the three nodes W, X, and Y in Fig. 6, in which W is the return node for j_z and the reference node for v_x and v_y. Such a group of nodes WXY will be described as a "test signal injection point," or simply an "injection point." A test signal injection point WXY is a dual injection point, a single current injection point, or a single voltage injection point.

It was mentioned at the end of the derivation that the GNT has the same format as the expression that describes the block diagram model of Fig. 3 or 4. Consequently, the same model can be shown with the blocks labeled in terms of a particular set of second-level transfer functions, as shown in Fig. 7.

The sequence of steps in arriving at the model of Fig. 7 exposes the benefits of the GNT. In the conventional approach, as reviewed in Section 1, the block diagram of Fig. 1 or 2 is *assumed*, and the gain expressions for the individual blocks are *guessed* in terms of the circuit structure. This is easy when the blocks are clearly separable, but becomes progressively more uncertain in the presence of nonidealities.

In contrast, with the GNT, the expressions for the individual blocks are *part of the answer*, and are *unambiguous;* there is no guesswork or uncertainty. Simplifications are optional in the symbolic analysis and not needed in the numerical analysis, but in any case are made with full knowledge of the degree of approximation, not forced in order to identify the blocks.

3. The General Feedback Theorem (GFT)

The block diagram of Fig. 7 models any transfer function of a circuit diagram regardless of any mention of "feedback," and can be considered a "natural" model. However, because the block diagram is the same form as in Fig. 3 or 4, it is particularly suited to represent a system in which there is an identifiable feedback loop, in which case the GNT is more usefully called a General Feedback Theorem (GFT). Although the equations are the same, some interpretations are more illuminating when slanted towards conventional single-loop feedback terminology.

For example, in Fig. 7 it is obvious that T is the "loop gain" and H_∞ is the ideal closed-loop gain as in Fig. 3 or 4. Thus, the second-level transfer function T, and its constituent third-level transfer functions, can be considered as *either* return ratios *or* loop gains and, by extension, the same applies to T_n.

A more detailed justification for this dual nomenclature is the following. The GFT is a special case of the EET in which the extra elements are the controlled current and/or voltage generators of one or more fictitious ideal transformers inserted into the system circuit model. The third-level transfer functions, the T's and T_n's, are return ratios of the controlled generators but, since the normal values of the controlled generators are unity, the T's and T_n's can also be identified as loop gains, and are calculated by test signal injection into the system circuit model (without the fictitious ideal transformers).

It is convenient at this point to summarize the general network theorem results interpreted as a General Feedback Theorem (GFT).

A particular test signal injection point produces a mutually consistent set of four second-level transfer functions H_∞, T, T_n, H_0 which comprise the first-level transfer function H. Owing to the redundancy relation $H_0 / H_\infty = T / T_n$ of (45), the GFT can be expressed in terms of three out of the four second-level transfer functions:

$$H = H_\infty \frac{1+\frac{1}{T_n}}{1+\frac{1}{T}} \qquad (59) \qquad\qquad H = H_\infty \frac{T}{1+T} + H_0 \frac{1}{1+T} \qquad (60)$$

in which T is the loop gain (total return ratio), T_n is the null loop gain (total null return ratio), H_∞ is the transfer function in the limit $T = \infty$, and H_0 is the transfer function in the limit $T = 0$. In (59), G_0 is absent, and in (60) T_n is absent; the other two versions, absent H_∞ and T respectively, are not shown.

For interpretation of the GFT, it is convenient to define two weighting factors so that (59) and (60) can be written

$$H = H_\infty D D_n \qquad (61) \qquad\qquad H = H_\infty D + H_0(1-D) \qquad (62)$$

where

$$D \equiv \frac{T}{1+T} \qquad (63) \qquad\qquad D_n \equiv \frac{1+T_n}{T_n} \qquad (64)$$

are respectively the "discrepancy factor" and the "null discrepancy factor." The term "discrepancy" is chosen because D represents the consequences of noninfinite loop gain, and D_n represents all the nonidealities, that cause the actual closed-loop gain H to differ from the ideal closed-loop gain H_∞.

In (61), the nonidealities are accounted for via D_n as a multiplier upon the basic single-loop $H_\infty D$, and in (62) they are accounted for via H_0 as an additive term to $H_\infty D$.

For dual test signal injection of j_z and e_z, these second-level transfer functions are given by (19) through (21):

Dual injection j_z and e_z:

$$H_\infty \equiv H^{i_y v_y} \qquad (65)$$

$$\frac{1}{T} \equiv \frac{1}{T_i^{v_y}} + \frac{1}{T_v^{i_y}} + \frac{1}{T_{iv}} \qquad (66)$$

$$\frac{1}{T_n} \equiv \frac{1}{T_{ni}^{v_y}} + \frac{1}{T_{nv}^{i_y}} + \frac{1}{T_{niv}} \qquad (67)$$

where the product terms T_{iv} and T_{niv} are given by (15) and (16):

$$T_{iv} \equiv T_i^{v_x} T_v^{i_y} = T_i^{v_y} T_v^{i_x} \qquad (68)$$

$$T_{niv} \equiv T_{ni}^{v_x} T_{nv}^{i_y} = T_{ni}^{v_y} T_{nv}^{i_x} \qquad (69)$$

The third-level transfer functions are the constituents of the second-level transfer functions, and are calculated from the circuit model according to (9) and (22) through (29).

For single test signal injection of j_z or e_z, the second-level transfer functions are obtained from (30) and (34) and are respectively equal to the third-level transfer functions calculated from the circuit model according to (38) through (43):

Current injection j_z :

$$H_\infty = H^{i_y} \qquad (70)$$

$$T = T_i \qquad (71)$$

$$T_n = T_{ni} \qquad (72)$$

Voltage injection e_z :

$$H_\infty = H^{v_y} \qquad (73)$$

$$T = T_v \qquad (74)$$

$$T_n = T_{nv} \qquad (75)$$

Any injection point, with either single or dual test signal injection, gives a mutually consistent set of second-level transfer functions that, when inserted into the GFT of any of the four versions (59) through (62), produces the same result for the closed-loop transfer function H. A designer has the option to choose an injection point so that the second-level transfer functions define blocks in the natural model of Fig. 7 that best match the actual physical circuit. This gives the designer maximum insight into the circuit operation and hence gives the greatest control over performance optimization.

There are two criteria to guide a designer's choice of injection point.

First, the whole signal in the forward path (in either direction), and none of the signal in the feedback path (in either direction), should pass through the test signal injection point. That is, the injection point should be inside the major loop,

the loop that is purposely constructed by the designer to achieve certain results, yet outside any minor loops that may be present either parasitically or on purpose to shape the major loop gain. Specifically, this means that in Fig. 5(a) signal transmission in the forward path is killed if branch XY is opened, or if node W is shorted to nodes X and Y.

Second, H_∞ should be equal to the desired ideal closed-loop gain $1/K$, the reciprocal of the feedback path transmission from the output back to the input. Satisfaction of these two criteria not only makes the overall block diagram model of Fig. 7 match that of Fig. 3 or 4, but it also makes the individual blocks match as well. Consequently, the second-level transfer functions H_∞, T, T_n, H_0 have the most useful design-oriented interpretations in terms of the circuit model.

The set of second-level transfer functions that satisfy both criteria may be called the "principal set," which includes the "principal loop gain" T. The injection point that produces the principal set describes not only the places where the test signals are injected, but also whether dual or single test signals are needed, according to whether $H^{i_y v_y}$, H^{i_y}, or H^{v_y} produces the desired $H_\infty = 1/K$.

Of course, this is not to suggest that other sets of second-level transfer functions are "wrong" in some way — they all give the same first-level closed-loop gain H — it is just that they are more distant from the physical circuit operation, and are therefore less useful for design purposes.

The crucial choice of test signal injection point is best illustrated by a circuit example, as in the following section.

4. Example: Two-Stage NonInverting Feedback Amplifier

An ac small-signal model of an elementary two-stage BJT feedback amplifier is shown in Fig. 8, in which the power supply line becomes ac ground.

Each BJT is represented by a core model of two elements, a controlled generator specifying the collector current to be α times the emitter current, and an emitter resistance $r_m = \alpha / g_m$, where g_m is the transconductance that represents the device gain property. Subscripts 1 and 2 identify the parameters of the two transistors. Augmenting each transistor core model is a collector-base capacitance C that represents the unavoidable transition-layer capacitance.

A benefit of the core model described above [11] is that it applies equally well to an FET. Apart from the obvious change in terminology, the only substantive change is in fact a simplification: for an FET, $\alpha = 1$, so that the base (now gate) current becomes zero. To take advantage of this simplification, both transistors will be taken to be FETs throughout this example, so r_m is the reciprocal transconductance and C is the drain-gate capacitance.

The GFT is used in Section 4.1 to derive the voltage gain G, with $H \to G$, and in Section 4.2 to derive the output impedance Z_o, with $H \to Z_o$.

4.1. Voltage Gain G

Some initial design choices are already implicit in Fig. 8. Qualitatively, the two FETs, both in common-source configuration, constitute the forward path; negative feedback is taken from the output voltage v_o via the divider $K = R_1 / (R_1 + R_2)$ and applied in series opposition with the input voltage e_i. Consequently, the circuit approximates a voltage-to-voltage amplifier with high input impedance and low output impedance, having a desired voltage gain of

$1/K = (R_1 + R_2)/R_1 = 20\text{dB}$, according to Design Step #1 of Section 1. Hence, the first-level transfer function H is now to be identified as the voltage gain $G \equiv v_o / e_i$.

The model of Fig. 8, simple though it appears, exhibits all the nonidealities previously discussed: mutual loading between the forward gain and feedback blocks; direct forward transmission; and two minor feedback loops created by the nonzero admittances across the controlled current generators.

The GFT is able to incorporate all these nonidealities, although the results for the second-level quantities depend upon the location of the injection point for the test signals j_z and/or e_z, and choice of the test signal injection point is critical to the usefulness of the results for design purposes. The preferred choice is an injection point that meets the two criteria described in the previous section, and produces the principal set of second-level transfer functions.

If the feedback loop is defined to be the major loop installed by the designer, the injection point should be inside the forward path but outside any minor loops, and such that all the signal in the forward path goes through that one point. Thus, the only signal that does not go through that point goes through the major loop feedback path. Points $W_1X_1Y_1$, $W_1X_2Y_2$, and $W_1X_3Y_3$ in Fig. 8 meet this requirement.

Also, the ideal closed-loop gain G_∞ should be equal to the reciprocal feedback divider ratio $1/K=(R_1 + R_2)/R_1$, which in turn means that both the "error voltage" between W_2 and Y_3 and the "error current" at the R_1, R_2 divider point must be zero. Therefore, the error current and error voltage must respectively be identified as i_y and v_y in order to make $G^{i_y v_y} = G_\infty$ equal to $(R_1 + R_2)/R_1$. Hence, both current and voltage test signals j_z and e_z must be injected at the X_3Y_3 branch with reference node W_2, as shown in Fig. 9.

Since the third-level loop gains are all calculated with e_i=0, it doesn't matter whether the reference node is W_1 or W_2. Therefore dual injection of both j_z and e_z at $W_2X_3Y_3$ meets both criteria and produces the principal set of G_∞, T, T_n, G_0 in which T is the principal loop gain. The consequences of other injection point choices will be considered later.

Figure 9 also shows some other modifications from Fig. 8: the two capacitances are generalized to impedances, the device αs are taken to be unity with resulting transistor input currents zero (if FETs) or ignored (if BJTs); and the source resistance R_s is taken to be zero. The last two greatly simplify the algebra of the GFT calculations without compromising the principles illustrated in the example. The consequences of nonzero R_s will also be briefly considered later.

An appropriate form of the GFT is therefore (59) or (60) and (65) with G replacing H:

$$G = G_\infty \frac{1 + \frac{1}{T_n}}{1 + \frac{1}{T}} \qquad (76) \qquad\qquad G = G_\infty \frac{T}{1+T} + G_0 \frac{1}{1+T} \qquad (77)$$

$$G_\infty = G^{i_y v_y} \qquad (78)$$

The scenario for implementation of the GFT is as follows: Determine the third-level quantities from the circuit, and calculate the second-level quantities from (66) and (67). These can be used directly for design purposes, or to calculate the first-level quantity G, the transfer function of interest. The implementation can be

realized by symbolic analysis, by a computer circuit simulator (preferably both), or (usually with considerably greater difficulty) by measurement on the physical circuit.

For the example of Fig. 9, symbolic analysis will be done, but first the results for the second-level quantities from a circuit simulator will be presented and assembled into the GFT to arrive at the first-level voltage gain transfer function G, which is then compared with the result by direct simulation.

All of the third-level quantities are multiple null injection calculations. Simulators are not set up to make such calculations, but this limitation can easily be overcome by adapting, not the simulator algorithm, but the circuit under test. For example, if two signals are to be nulled by mutual adjustment of three independent sources, two sources are replaced by controlled generators each driven by one of the signals to be nulled, and assigned very high gains. Thus, there is one independent source, and the two nulls are automatically created by self-adjustment of the two controlled generators; the simulator then calculates the required transfer function in the usual way. Intusoft's ICAP/4 IsSpice circuit simulator has a special GFT subprogram in which the user has only to specify the injection point and the type of test signal injection (current, voltage, or both), and the frequency responses of all the third-, second-, and first level transfer functions are made available.

Partial results for the circuit of Fig. 9, printed out by ICAP/4's IntuScope, are shown in Fig. 10. The final closed-loop gain G according to the GFT, calculated from (76), is compared with that obtained by direct simulation of v_o / e_i.

It is seen that the result from the GFT is indistinguishable from that obtained by direct simulation.

Useful insight is achieved by examination of the second-level quantities that constitute the GFT according to (76). The loop gain T is large at low frequencies but falls off and crosses 0dB at about 32MHz. The ideal closed-loop gain G_∞ has the designed flat value 20dB, and the closed-loop gain G follows at low frequencies but falls below G_∞ beyond the loop gain crossover frequency.

In Fig. 10, the closed-loop gain G actually rises before falling, exhibiting almost a 6dB peak. Viewed in isolation, as it would be if the GFT were not invoked, this peaking might be attributed to a low phase margin of about 30° with consequent step response having significant overshoot and ringing.

In fact, this does not happen, and the actual step response is very different. As can be seen from Fig. 10, loop gain crossover occurs well inside several decades of approximately -20dB/dec slope, indicating a phase margin of about 90°. The culprit is T_n, which crosses 0dB before T does. One of the principal benefits of the GFT is the insight afforded into how the second-level transfer functions, such as T_n, are determined by the circuit elements, so that any corrective action can be taken.

All the third-level quantities to be derived by analysis of the model of Fig. 9 are multiple null injection calculations for which, as already mentioned, the "short-cut" method of following the signal from "input" to "output" is particularly appropriate. The form of result desired for each transfer function is a reference value modified by pole and zero factors, the "factored pole-zero" format. Especially important is that the reference value and the poles and zeros be expressed in low entropy forms, that is, the element values should appear in ratios and series-parallel combinations. This is so that each result can be traced back to its origin in particular circuit elements and can be appropriately modified in an informed way as part of the design process. This is the essence of "design-oriented analysis," the only kind of analysis worth doing [10].

The various third-level transfer functions for the model of Fig. 9 will now be derived. Since several of them involve the current transfer function $M \equiv i / i_x$, in the long run work is saved by calculation of this transfer function in advance. Furthermore, since M in turn involves the only two complex impedances in the model, a convenient analysis tool is the 2EET in which the two impedances are reinstated by a correction factor upon a reference model in which the two impedances are absent. This takes advantage of the valuable special case when all the reactances in the circuit model are designated as extra elements, because then the transfer function reference value is a constant, all the driving point impedances are resistances, and the entire frequency response emerges automatically as a ratio of polynomials in complex frequency s, which can then be factored into the poles and zeros.

The relevant part of Fig. 9 is shown in Fig. 11, in which the reference values of the two impedances are infinite. The load resistance R of the second stage ultimately will be identified as either R_2, $R_1 + R_2$, or 0 according to which third-level transfer function is being calculated. The corresponding version of the 2EET is

$$M \equiv M\big|_{Z_1, Z_2 = \infty} \frac{1 + \frac{R_{n1}}{Z_1} + \frac{R_{n2}}{Z_2} + K_n \frac{R_{n1}}{Z_1}\frac{R_{n2}}{Z_2}}{1 + \frac{R_{d1}}{Z_1} + \frac{R_{d2}}{Z_2} + K_d \frac{R_{d1}}{Z_1}\frac{R_{d2}}{Z_2}} \tag{79}$$

where the "interaction parameters" K_d and K_n are given by

$$K_d \equiv \frac{R_{d1}\big|_{Z_2=0}}{R_{d1}} = \frac{R_{d2}\big|_{Z_1=0}}{R_{d2}} \tag{80}$$

$$K_n \equiv \frac{R_{n1}\big|_{Z_2=0}}{R_{n1}} = \frac{R_{n2}\big|_{Z_1=0}}{R_{n2}} \tag{81}$$

From Fig. 11, it is seen immediately that the reference value of M is

$$M\big|_{Z_1, Z_2 = \infty} = \frac{R_3}{r_{m2}} \tag{82}$$

To find the eight driving point resistances, the procedure is to redraw Fig. 11 with the appropriate quantities to be nulled explicitly marked to zero. Since there are many such procedures to be accomplished, too much space would be needed to display all the redrawn versions of Fig. 11. Instead, Fig. 11 can be considered a "template" from which copies can be made to be marked up with the appropriate signal values.

$\boldsymbol{R_{d1}}$

Redraw Fig. 11 with a test source (current or voltage) applied between terminals 1,1′, and with the "input" signal i_x (denominator of M) set to zero: call this Fig. 11.1. The driving point resistance seen by the test source is R_{d1} which, because i_x=0 and the input current to the second stage is zero, is

$$R_{d1} = R_3 \tag{83}$$

$\boldsymbol{R_{d1}\big|_{Z_2=0}}$

Redraw Fig. 11.1 with terminals 2,2′ short instead of open: call this Fig. 11.2. The driving point resistance seen by the test source is :

$$R_{d1}\big|_{Z_2=0} = r_{m2} \| R \| R_3 \tag{84}$$

$\boldsymbol{R_{n1}}$

Redraw Fig. 11 with a test source applied between terminals 1,1′, and with the "output" signal i (numerator of M) nulled (in the presence of i_x): call this Fig. 11.3. Since i=0, i_2 is also zero, and there is zero voltage across the test source. Therefore

$$R_{n1} = 0 \tag{85}$$

$\boldsymbol{R_{n1}}\big|_{Z_2=0}$

Redraw Fig. 11.3 with terminals 2,2′ short instead of open: call this Fig. 11.4. Since there was no voltage across terminals 2,2′ under the conditions of Fig. 11.3, the result is the same whether terminals 2,2′ are open or short, hence

$$R_{n1}\big|_{Z_2=0} = 0 \tag{86}$$

$\boldsymbol{R_{d2}}$

Redraw Fig. 11 with a test current i_t applied between terminals 2,2′, and with the "input" signal i_x set to zero: call this Fig. 11.5. The test current i_t also flows through R_3, so $i_2 = (R_3 / r_{m2})i_t$ and $i = i_2 + i_t$. The driving point resistance R_{d2} is the sum of the voltages across R_3 and R divided by i_t, so

$$R_{d2} = R_3 + \left(1 + \frac{R_3}{r_{m2}}\right)R = \frac{RR_3}{r_{m2}\|R\|R_3} \tag{87}$$

$\boldsymbol{R_{d2}}\big|_{Z_1=0}$

Redraw Fig. 11.5 with terminals 1,1′ short instead of open: call this Fig. 11.6. Since there is zero voltage across r_{m2}, i_2=0 and

$$R_{d2}\big|_{Z_1=0} = R \tag{88}$$

$\boldsymbol{R_{n2}}$

Redraw Fig. 11 with a test source applied between terminals 2,2′, and with the "output" signal i (numerator of M) nulled (in the presence of i_x): call this Fig. 11.7. Since i=0, i_2 flows through the test source and the voltage across it is $-r_{m2}i_2$, so

$$R_{n2} = -r_{m2} \tag{89}$$

$\boldsymbol{R_{n2}}\big|_{Z_1=0}$

Redraw Fig. 11.7 with terminals 1,1′ short instead of open: call this Fig. 11.8. Conditions are the same as for R_{n2} regardless of whether terminals 1,1′ are short or open, so

$$R_{n2}\big|_{Z_1=0} = -r_{m2} \tag{90}$$

With all eight driving point resistances determined, the redundant definitions of K_d and K_n can be checked. Both versions of (80) give

$$K_d = \frac{r_{m2}\|R\|R_3}{R_3} \tag{91}$$

The first version of (81) gives zero over zero and is indeterminate, but the second version gives

$$K_n = 1 \tag{92}$$

Consequently, because $K_d \neq 1$, the denominator of (79) does not factor exactly, but because K_n=1, the numerator does (although one factor is unity because R_{n1}=0).

With insertion of the various components into (79), the result for M is

$$M = \frac{R_3}{r_{m2}} \frac{1 - \frac{r_{m2}}{Z_2}}{1 + \frac{R_3}{Z_1} + \frac{R}{r_{m2} \| R \| R_3} \frac{R_3}{Z_2} + \frac{R}{Z_1} \frac{R_3}{Z_2}} \tag{93}$$

With an expression for M in hand, analysis for the third-level transfer functions can proceed with dispatch. Since there are several such analyses to be done, Fig. 9 can also be considered a "template" circuit diagram from which copies can be made to be marked up with the appropriate signal values.

$\boldsymbol{G^{i_y v_y}}$

Figure 9 does not have to be redrawn to recognize that with v_y nulled the input voltage e_i appears across R_1, and with i_y nulled the current through R_2 is the same as that through R_1, and so the output voltage v_o is the reciprocal feedback divider ratio times the input voltage e_i, and

$$G^{i_y v_y} = \frac{R_1 + R_2}{R_1} \tag{94}$$

Of course, this is not a surprise since the injection point was specifically chosen to set up this result.

There are eight third-level return ratios needed to obtain the two second-level return ratios T and T_n defined by (66) through (69). The easiest ones will be disposed of first.

$\boldsymbol{T_i^{v_x}, T_v^{i_x}, T_{ni}^{v_x}, T_{nv}^{i_x}}$

In the circuit of Fig. 9, $v_x = r_{m1} i_x$ under all conditions, so if either signal is nulled, the other is also zero. Therefore, the denominators of (23), (25), (27) and (28) are all zero, and consequently

$$T_i^{v_x}, T_v^{i_x}, T_{ni}^{v_x}, T_{nv}^{i_x} = \infty \tag{95}$$

This would not be the case if R_s were not zero, so adoption of R_s=0 enables a considerable simplification.

$\boldsymbol{T_i^{v_y}}$

Redraw Fig. 9 with e_i set to zero, and v_y marked zero (nulled): call this Fig. 9.1. There is therefore zero voltage across R_1, so $i = i_y$. But $i = M i_x$, where M is given by (93) with $R \to R_2$ (because of zero voltage across R_1). Hence

$$T_i^{v_y} = M|_{R \to R_2} = \frac{R_3}{r_{m2}} \frac{1 - \frac{r_{m2}}{Z_2}}{1 + \frac{R_3}{Z_1} + \frac{R_2}{r_{m2} \| R_2 \| R_3} \frac{R_3}{Z_2} + \frac{R_2}{Z_1} \frac{R_3}{Z_2}} \tag{96}$$

$\boldsymbol{T_v^{i_y}}$

Redraw Fig. 9 with e_i set to zero, and i_y marked zero (nulled): call this Fig. 9.2. Because i_y=0, the current through R_1 is i and $v_y = R_1 i$. Also, $v_x = r_{m1} i_x$, so $v_y / v_x = (R_1 / r_{m1})(i / i_x)$. But $(i / i_x) = M$, where M is given by (93) with $R \to R_1 + R_2$ (because i_y=0). Hence

$$T_v^{i_y} = M|_{R\to R_1+R_2} = \frac{R_3}{r_{m2}} \frac{1-\dfrac{r_{m2}}{Z_2}}{1+\dfrac{R_3}{Z_1}+\dfrac{R_1+R_2}{r_{m2}\|(R_1+R_2)\|R_3}\dfrac{R_3}{Z_2}+\dfrac{R_1+R_2}{Z_1}\dfrac{R_3}{Z_2}} \tag{97}$$

$\boldsymbol{T_{ni}^{v_y}}$

Redraw Fig. 9 with both v_y and v_o marked zero (nulled, in the presence of nonzero e_i); call this Fig. 9.3. By the analysis leading to (93), i was found in terms of i_x with e_i zero; in Fig. 9.3 e_i is not zero but, by formation of a Norton equivalent of e_i and Z_1, contributes an additional component e_i / Z_1 to the controlled generator labeled i_x. Thus,

$$i = M|_{R\to 0}\left(i_x + \frac{e_i}{Z_1}\right) \tag{98}$$

where $M|_{R\to 0}$ is given by (93) with $R \to 0$ because the output voltage v_o is nulled. This gives i_x as

$$i_x = \frac{i}{M|_{R\to 0}} - \frac{e_i}{Z_1} \tag{99}$$

whose interpretation is that i_x supplies only the part of i that is not provided by e_i. Also from Fig. 9.3, with use of the nulled v_y and v_o, the current i determines both e_i and i_y as $e_i = R_2 i$ and $i_y = e_i / \left(R_1 \| R_2\right)$, so (99) becomes

$$\frac{1}{T_{ni}^{v_y}} = \frac{R_1}{R_1+R_2}\left(\frac{1}{M|_{R\to 0}} - \frac{R_2}{Z_1}\right) \tag{100}$$

A little straightforward algebra then leads to

$$T_{ni}^{v_y} = \frac{R_1+R_2}{R_1}\frac{R_3}{r_{m2}} \frac{1-\dfrac{r_{m2}}{Z_2}}{1-\left(\dfrac{R_2}{r_{m2}}-1\right)\dfrac{R_3}{Z_1}+\dfrac{R_3}{Z_2}+\dfrac{R_2}{Z_1}\dfrac{R_3}{Z_2}} \tag{101}$$

$\boldsymbol{T_{nv}^{i_y}}$

Redraw Fig. 9 with both i_y and v_o marked zero (nulled, in the presence of nonzero e_i); Call this Fig. 9.4. Because R_1 and R_2 are in parallel (v_o=0) and the current through them is i_y=0, i=0 also. Therefore, i_2 flows through Z_2 and, because v_o=0, $Z_2 i_2 = r_{m2} i_2$ and i_2=0 also. There is therefore no current in R_3, so i_x flows through Z_1 and, since e_i appears across Z_1, $e_i = Z_1 i_x$ (this argument could be shortened). Finally, $v_y = e_i$ (because of zero current in R_1), and $i_x = v_x / r_{m1}$, so

$$T_{nv}^{i_y} = -\frac{Z_1}{r_{m1}} \tag{102}$$

This completes the symbolic analysis for all the results for the third-level quantities needed to find the second-level transfer functions G_∞, T, and T_n in (76). Since $T_i^{v_x}$ and $T_v^{i_x}$ are both infinite, the product term T_{iv} of (68) is also infinite, and so by (66) T reduces to the parallel combination of $T_i^{v_y}$ and $T_v^{i_y}$, and likewise for T_n by (67).

From (66) and (67), for the element values in Fig. 8 (R_s=0), it can be determined that for all frequencies T and T_n are dominated respectively by $T_i^{v_y}$ and $T_{ni}^{v_y}$. An even easier way to reach this conclusion is to use the ICAP/4 GFT subprogram to plot all four constituent third-level transfer functions, as shown in Fig. 12, from which it is seen that $T_v^{i_y}$ and $T_{nv}^{i_y}$ are negligibly large. However, only a little algebra is required to produce the exact parallel combinations:

$$T = \frac{R_3}{r_{m2}} \frac{1}{1+\frac{r_{m1}}{R_1}} \frac{1-\frac{r_{m2}}{Z_2}}{1+\frac{R_3}{Z_1}+\left(\frac{R_2+r_{m1}\|R_1}{r_{m2}\|\left(R_2+r_{m1}\|R_1\right)\|R_3}\right)\frac{R_3}{Z_2}+\frac{R_2+r_{m1}\|R_1}{Z_1}\frac{R_3}{Z_2}} \tag{103}$$

$$T_n = \frac{R_1+R_2}{R_1} \frac{R_3}{r_{m2}} \frac{1-\frac{r_{m2}}{Z_2}}{1-\left[\frac{R_2}{r_{m2}}\left(1+\frac{r_{m1}}{R_1\|R_2}\right)-1\right]\frac{R_3}{Z_1}+\frac{R_3}{Z_2}+\left(1+\frac{r_{m1}}{R_1\|R_2}\right)\frac{R_2}{Z_1}\frac{R_3}{Z_2}} \tag{104}$$

Two sets of approximations are available. First, for the (good) approximation $r_{m1} << R_1\|R_2$ (which also validates $r_{m1} << R_1$ and $r_{m1}\|R_1 << R_2$), comparison of (96) with (103) and of (101) with (104) shows that $T \approx T_i^{v_y}$ and $T_n \approx T_{ni}^{v_y}$, as confirmed by comparison of Figs. 10 and 12.

Second, for the element values in Fig. 8, further simplification of the results for T and T_n can be accomplished. For T, the Z_1 term can be dropped with less than 6% error, and the paralleling effect of $R_2\|R_3$ upon r_{m2} is completely negligible, and so a simpler version of (103) is

$$T \approx \frac{R_3}{r_{m2}} \frac{1-\frac{r_{m2}}{Z_2}}{1+\frac{R_2}{r_{m2}}\frac{R_3}{Z_2}+\frac{R_2}{Z_1}\frac{R_3}{Z_2}} \tag{105}$$

For T_n, there is less than 0.3% error in dropping the -1 inside the bracket, and even less error in dropping the R_3 / Z_2 term, and so a simpler version of (104) is

$$T_n \approx \frac{R_1+R_2}{R_1} \frac{R_3}{r_{m2}} \frac{1-\frac{r_{m2}}{Z_2}}{1-\frac{R_2}{r_{m2}}\frac{R_3}{Z_1}+\frac{R_2}{Z_1}\frac{R_3}{Z_2}} \tag{106}$$

It remains to put these results in factored pole-zero form.

The denominator Den$T$ of (105) is of the form

$$\text{Den}T = 1+\frac{1}{Q}x+x^2 \tag{107}$$

which factors to

$$\text{Den}T = \left(1+\frac{F}{Q}x\right)\left(1+\frac{Q}{F}x\right) \tag{108}$$

where

$$F = \tfrac{1}{2}+\tfrac{1}{2}\sqrt{1-4Q^2} \tag{109}$$

For the element values in Fig. 8, F= 0.999,986 so the error in taking F=1 is utterly negligible — in exchange for the huge benefit of banishing the radical sign from the famous quadratic root formula [12]. Consequently, (105) can be written

$$T = \frac{R_3}{r_{m2}} \frac{1 - \frac{r_{m2}}{Z_2}}{\left(1 + \frac{R_2}{r_{m2}} \frac{R_3}{Z_2}\right)\left(1 + \frac{r_{m2}}{Z_1}\right)} \tag{110}$$

Substitution of Z_1 and Z_2 in terms of the corresponding capacitances discloses a two-pole, one-zero form:

$$T = T(0) \frac{\left(1 - \frac{s}{\omega_{z1}}\right)}{\left(1 + \frac{s}{\omega_{p1}}\right)\left(1 + \frac{s}{\omega_{p2}}\right)} \tag{111}$$

where

$$T(0) = \frac{R_3}{r_{m2}} = 4.00 \times 10^3 \Rightarrow 72\text{dB} \tag{112}$$

$$\omega_{p1} = \frac{1}{C_2 R_2} \frac{r_{m2}}{R_3}; \qquad f_{p1} = 8.8\text{kHz} \tag{113}$$

$$\omega_{p2} = \frac{1}{C_1 r_{m2}}; \qquad f_{p2} = 640\text{MHz} \tag{114}$$

$$\omega_{z1} \equiv \frac{1}{C_2 r_{m2}}; \qquad f_{z1} = 13\text{GHz} \tag{115}$$

These salient features agree with the graph obtained by ICAP/4 in Fig. 10.

It is convenient to expose the loop gain crossover frequency ω_c in the leading coefficient, by inversion of the lower pole in (111):

$$T = \frac{\omega_c}{s} \frac{\left(1 - \frac{s}{\omega_{z1}}\right)}{\left(\frac{\omega_{p1}}{s} + 1\right)\left(1 + \frac{s}{\omega_{p2}}\right)} \tag{336}$$

where

$$\omega_c \equiv \frac{1}{C_2 R_2}; \qquad f_c = 35\text{MHz} \tag{117}$$

The simulated value in Fig. 10 is f_c=32MHz, which is the value obtained from (103) without the numerical approximations leading to (117).

A similar procedure upon the null loop gain T_n of (323a) produces a denominator factorization in which the second pole cancels the zero, with the result

$$T_n = \frac{R_1 + R_2}{R_1} \frac{R_3}{r_{m2}} \frac{1}{1 - \frac{R_2}{r_{m2}} \frac{R_3}{Z_1}} \tag{118}$$

In factored pole-zero form

$$T_n = T_n(0) \frac{1}{\left(1 - \frac{s}{\omega_{zn}}\right)} \tag{119}$$

where

$$T_n(0) \equiv \frac{R_1 + R_2}{R_1}\frac{R_3}{r_{m2}} = 40{,}000 \Rightarrow 92\text{dB} \tag{120}$$

$$\omega_{zn} \equiv \frac{1}{C_1 R_2}\frac{r_{m2}}{R_3}; \qquad f_{zn} = 440\text{Hz} \tag{121}$$

Again, inversion of the pole exposes the null loop gain crossover frequency ω_{nc}:

$$T_n = \frac{\omega_{nc}}{s}\frac{1}{\left(\frac{\omega_{zn}}{s} - 1\right)} \tag{122}$$

where

$$\omega_{nc} = \frac{1}{C_1 R_2}\frac{R_1 + R_2}{R_1}; \qquad f_{nc} = 18\text{MHz} \tag{123}$$

The analysis results for T_n also agree with the ICAP/4 graph in Fig. 10.

Factored pole-zero forms for the discrepancy factors D and D_n can be found by substitution of (111) and (119) into (63) and (64) , but the results can be written down simply by inspection of Fig. 10: D is 0dB until the T crossover frequency ω_c, and then follows T downwards. Likewise, D_n is 0dB until the T_n crossover frequency ω_{nc} and then follows $1/T_n$ upwards:

$$D = \frac{\left(1 - \frac{s}{\omega_{z1}}\right)}{\left(1 + \frac{s}{\omega_c}\right)\left(1 + \frac{s}{\omega_{p2}}\right)} \tag{124}$$

$$D_n = \left(1 - \frac{s}{\omega_{nc}}\right) \tag{125}$$

The product of G_∞= 20dB with (124) and (125) then gives the final first-level transfer function G from (61):

$$G = G_\infty \frac{\left(1 - \frac{s}{\omega_{nc}}\right)\left(1 - \frac{s}{\omega_{z1}}\right)}{\left(1 + \frac{s}{\omega_c}\right)\left(1 + \frac{s}{\omega_{p2}}\right)} \tag{126}$$

The product $G_\infty D$ and D_n are shown separately in Fig. 13. The final triple product is the G already shown in Fig. 10, whose structure is now clear. The loop gain T has almost a 90° phase margin (the phase of T is the same as the phase of $T_i^{v_y}$ in Fig. 12(a)), so there is no peaking in D as confirmed by Fig. 13. The apparent peaking of G is actually a shelf caused by the crossover frequency of T_n being lower than that of T. The height of the shelf above G_∞ is ω_c / ω_{nc} which, from (117) and (123), is

$$\frac{\omega_c}{\omega_{nc}} = \frac{C_1}{C_2}\frac{R_1}{R_1 + R_2} = 2 \Rightarrow 6\text{dB} \tag{127}$$

Consequently, as displayed in Fig. 14, the response of the model of Fig. 8 to an input step of 1V does not exhibit overshoot and ringing, but instead shows a huge undershoot. There is an initial output step of +1V before the undershoot begins.

The C_1/C_2 ratio of 20:1 in the circuit model of Fig. 8 was purposely chosen to expose the apparent peaking in the closed-loop gain G which, in the absence of the second-level quantities, might erroneously be ascribed to a low phase margin. From

a design perspective, the shelf in the closed-loop gain G could be eliminated by decreasing the ratio C_1 / C_2. However, this does little for the undershoot because G still has two poles and two rhp zeros.

The various nonidealities, via T_n, show up in the GFT of (61) as a multiplier factor D_n. A different perspective can be obtained from (62), in which the nonidealities, via G_0, show up as an additive term. Since the other three second-level transfer functions are already known in factored pole-zero form, G_0 is immediately obtained from (78), 316), (111), and (119) substituted into the redundancy relation (45) as

$$G_0 = \frac{\left(1-\frac{s}{\omega_{zn}}\right)\left(1-\frac{s}{\omega_{z1}}\right)}{\left(1+\frac{s}{\omega_{p1}}\right)\left(1+\frac{s}{\omega_{p2}}\right)} \tag{128}$$

The weighting factor (1-D) and G_0 are shown in Fig. 15, and the two products $G_\infty D$ and $G_0(1-D)$ are shown in Fig. 16, the sum of which is the G of Fig. 10. Both Figs. 13 and 16 show that the closed-loop gain G follows $G_\infty D$ at low frequencies, but that the nonidealities take over above the null loop gain crossover frequency ω_{nc}.

Since G_0 was found as a combination of the other three second-level transfer functions, its origin in the circuit model is obscure. This can be remedied by finding G_0 independently from (49), in which the first term is dominant and therefore, since $T \approx T_i^{v_y}$, $G_0 \approx G^{v_y i_x}$. By redrawing the template of Fig. 9 with v_y and i_x nulled, it can be seen that e_i reaches v_o by two parallel paths: a feedforward through the feedback path R_2, and a feedforward through the normal forward path via the local feedback path Z_1. The detailed derivation leads, with suitable numerical approximations, to (128), in which the first path dominates up to the first corner frequency and the second path dominates thereafter. Consequently, since by Fig. 16 the nonidealities do not take over until the much higher frequency ω_{nc}, the feedforward via Z_1 is the only nonideality that significantly affects the closed-loop gain G.

4.2 Output Impedance Z_o.

It has been reiterated several times that the GFT applies to any first-level transfer function of a linear system model, so as an example of a transfer function other than a voltage gain it will be applied to the output impedance Z_o of the circuit model of Fig. 8. Thus, H in Section 3 is replaced by Z_o.

The template model for the various calculations is the same as Fig. 9, except that e_i is permanently shorted and a new current source j_i is placed across the output port. The output impedance Z_o is the transfer function v_o / j_i, whose "input" is j_i and whose "output" is v_o.

The template model can be redrawn to set up the sets of conditions necessary to calculate the third-level quantities. The procedure is the same as for the voltage gain G, and so only the results will be given here.

First, it is seen that all the T's are the same as for the voltage gain G. This is because all the T's are calculated with zero "input", so it doesn't matter whether the

input is e_i or j_i. This is consistent with the fact that the natural poles of the system are independent of the location of the excitation.

Second, it is found that $Z_o^{i_y v_y}=0$ and $T_n=0$. Consequently, $Z_{o\infty}$ is zero and (59) cannot be used; instead, the GFT version of (60) or (62) is available with only the second term remaining:

$$Z_o = Z_{o0}\frac{1}{1+T} = Z_{o0}(1-D) \tag{129}$$

The component Z_{o0} has to be found from (49), rather than from (45) and, because $T_{iv}=\infty$, only two terms remain:

$$Z_{o0} = Z_o^{v_y i_x}\frac{T}{T_i^{v_y}} + Z_o^{i_y v_x}\frac{T}{T_v^{i_y}} \tag{130}$$

Because $Z_o^{v_y i_x}$ and $Z_o^{i_y v_x}$ are found to be comparable, and because it is already known that $T_v^{i_y} >> T_i^{v_y}$ so $T \approx T_i^{v_y}$, (130) reduces to

$$Z_{o0} \approx Z_o^{v_y i_x} \tag{131}$$

From Fig. 9 with $e_i=0$ and v_y and i_x nulled, the open-loop output impedance Z_{o0} is seen to be R_2 in parallel with the output impedance of the second stage. The resulting factored pole-zero form is

$$Z_{o0} = R_2\frac{\left(1+\dfrac{s}{\omega_{z2}}\right)}{\left(1+\dfrac{s}{\omega_{p1}}\right)\left(1+\dfrac{s}{\omega_{p2}}\right)} \tag{132}$$

where ω_{p1} and ω_{p2} are the same as in (113) and (114), and

$$\omega_{z2} \equiv \frac{1}{(C_1+C_2)R_3}; \qquad f_{z2} = 150\text{kHz} \tag{133}$$

The final assembly into (129) is shown in Fig. 17. As expected, the closed-loop output impedance Z_o is low at low frequencies, rises as the loop gain T declines, and becomes equal to the open-loop value Z_{o0} above loop-gain crossover at ω_c.

5. Discussion

One of the most beneficial features of the GFT is that the "bottom up" and the "top down" approaches come together in the natural block diagram model of Fig. 7, in which the blocks are individually defined in terms of the set of second level transfer functions that are exact results of analysis of the detailed circuit diagram. As already seen, the principal set is particularly useful because the test signal injection point is chosen to make $H_\infty = 1/K$, the reciprocal feedback ratio, and the corresponding T is the principal loop gain.

At the same time, the $H_\infty T$ block in Fig. 7 matches the open-loop forward gain block A in Figs 1 through 4. With respect to the example feedback amplifier of Fig. 8, in which H_∞ is replaced by $G_\infty = G^{i_y v_y}$ from (94) and the exact T from (103), the result is

$$A = A\big|_{Z_1,Z_2\to\infty} \frac{1-\dfrac{r_{m2}}{Z_2}}{1+\dfrac{R_3}{Z_1}+\left(\dfrac{R_2+r_{m1}\|R_1}{r_{m2}\|\left(R_2+r_{m1}\|R_1\right)\|R_3}\right)\dfrac{R_3}{Z_2}+\dfrac{R_2+r_{m1}\|R_1}{Z_1}\dfrac{R_3}{Z_2}} \tag{134}$$

where

$$A\big|_{Z_1,Z_2\to\infty} \equiv \frac{R_3}{r_{m1}+R_1}\frac{R_1+R_2}{r_{m2}} \tag{135}$$

and the second factor is recognized from (93) as the frequency dependent part of M with the effective load resistance equal to $R_2 + r_{m1}\|R_1$.

Might the forward gain block A have been "guessed" directly from the Fig. 8 circuit model?

One could postulate the following:

$$A = -\frac{\text{2nd stage drain load}}{\text{1st stage source load}}\ \frac{i}{i_1} \tag{136}$$

in which i/i_1 may be solved as $M=i/i_x$ from Fig. 9 as has already been done in (93) with $-i_1$ replacing i_x. There is already an implicit approximation: the feedforward through C_1 is omitted, and would have to be accounted for separately as part of the G_0 block.

The guesswork arises in assigning values to the 1st stage source load, the 2nd stage drain load, and the effective load R inside M, all with the feedback "disconnected." Possible choices are: 1st stage source load = $r_{m1} + R_1\|R_2$, as though v_o were shorted to ground; 2nd stage drain load and $R = R_2 + r_{m1}\|R_1$, as though e_i were shorted.

Insertion of these choices into (136) does indeed produce (134). It is also possible to "guess" the direct forward transmission block G_0, but the argument is even longer and more strained than that for A, and will not be given here. In any case, it is hard to justify these choices *a priori* without knowing the correct answer in advance, and so it seems highly preferable to interpret the GFT results in terms of the physical circuit operation, rather than to derive the results from a block diagram based on a possibly erroneous dissection of the actual circuit.

This is equivalent to saying that it is preferable to define K and A in terms of the GFT solution for H_∞ and T, rather than to define H_∞ and T in terms of K and A as would be done in a conventional approach.

In conventional analysis, it is common to eliminate the block G_0 in the model of Fig. 2 by modifying one or both of the remaining two blocks in such a way as to preserve the "right" answer for G. This can also be accomplished for Fig. 7, and one possible choice is to keep the K block the same and incorporate the H_0 block (in terms of T_n) into a modified A block, as shown in Fig. 18. This model has a closed-loop response

$$H = \frac{A_p}{1+T_p} \tag{137}$$

where T_p and A_p are respectively a "pseudo loop gain" and a "pseudo open-loop forward gain" defined by equating (137) with the GFT of (59):

$$T_p \equiv T\frac{1+\dfrac{1}{T_n}}{1-\dfrac{T}{T_n}} \tag{138}$$

$$A_p \equiv H_\infty T_p \tag{139}$$

Figure 18 can hardly be considered a "natural model," because the pseudo loop gain is a combination of two of the set of GFT second-level transfer functions and is hard to interpret directly in terms of the circuit elements.

If the pseudo loop gain T_p is evaluated for the example circuit of Fig. 8, it is found to have a crossover frequency different from T, and a much lower phase margin.

Another, simpler example is the integrator treated by Hurst [13]. In Fig. 6(a) of [13], the output of the forward path is represented by a Thevenin equivalent, and a test voltage e_z injected in series with the Thevenin controlled generator sets up a virtual ground at the feedback summing point that makes H_∞ (a transimpedance in this case) equal to the reactance $1/sC_F$ of the integrating capacitance, as desired. The corresponding principal T and T_n can easily be found (by inspection, in fact) from the circuit diagram. The result for T is the same as Eq. (24) and Fig. 6(c) of [13]. The pseudo loop gain T_p from (138) is the same as Eq. (23) and Fig. 6(b) of [13], but its interpretation in terms of the circuit elements is not so obvious.

The detailed treatment in Section 4 of the example circuit of Fig. 8 was for the two injection point criteria that establish G_∞, T, T_n, and G_0 as the principal set of second-level transfer functions, namely that test signal injection should be inside the major loop but outside any minor loops, and that G_∞ should equal the desired $1/K$. This is achieved by dual injection of both current and voltage test signals at $W_2X_3Y_3$, as shown in Fig. 9. It is of interest to see how the results differ when other injection choices are made.

Since T and T_n are both dominated by their respective current return ratios, it might be thought that in Fig. 9 only current injection j_z might be needed, with e_z zero throughout. Indeed, the results for G_∞, T, and T_n of Fig. 10 are unchanged, but only up to about 100MHz (half a decade above the loop gain crossover frequency of 32MHz); all three graphs deviate significantly at higher frequencies. In particular, G_∞ acquires two rhp zeros and a complex pair of poles that cause, at 680MHz, a peak of 7dB above its flat value of 20dB. The calculations are not only more complicated, but their interpretations in terms of the circuit properties are more strained, making them less useful for design purposes.

If only voltage injection e_z is employed in Fig. 9, with j_z zero throughout, the results are completely useless: T and T_n are both much greater than unity at all frequencies, so $G = G_\infty$ and all the work has to be done at once.

Thus for single injection of either j_z or e_z in Fig. 9, G_∞ is not equal to $1/K$ and the loop gain is not the principal loop gain.

Other injection points may be considered, for example dual test signal injection at $W_1X_1Y_1$ in Fig. 8. Again, G_∞ is the same as in Fig. 10, but only up to about 18MHz, which is the frequency of an rhp zero acquired by G_∞, and so G_∞ is not equal to $1/K$. The null loop gain T_n also differs from that in Fig. 10 above 18MHz. On the other hand T remains the same as in Fig. 10 at all frequencies

(although the third-level constituents are different), and so T is still the principal loop gain. The same is true for both current and voltage test signal injection at $W_1X_2Y_2$, and in fact all four second-level transfer functions G_∞, T, T_n, and G_0 are the same as for dual injection at $W_1X_1Y_1$. This demonstrates that the principal loop gain can be obtained for any dual injection point that is inside the major loop but outside the minor loops, although G_∞, T_n, and G_0 may be different from their values in the principal set.

Another choice would be current test signal j_z injection at $W_1X_1Y_1$, with e_z set to zero throughout. The loop gain $T=T_i$ is the same as in Fig. 10 up to the crossover frequency 35MHz. This is to be expected because C_1 is effectively an open over this frequency range, validating $W_1X_1Y_1$ as a current injection point at the output of a controlled current generator, as discussed in [4]. However, at higher frequencies this validation fails and both G_∞ and T deviate grossly from their shapes in Fig. 10.

Yet another choice would be voltage test signal e_z injection at $W_1X_1Y_1$, with j_z set to zero throughout. There is no frequency range over which this injection point is validated as a voltage injection point at the output of a controlled voltage generator, and so $T=T_v$ is nowhere the same as T in Fig. 10. It may be noted that the product $T_i T_v \approx 1$ at frequencies above loop gain crossover. This necessary result was also discussed in [4].

Thus again, if either j_z or e_z is zero in the injection point $W_1X_1Y_1$, G_∞ is not equal to $1/K$ and the loop gain is not the principal loop gain.

All the above variations have been related to whether or not an injection point produces a principal set of second-level transfer functions, including a principal loop gain. However, all loop gains are return ratios, and the return ratio for any component in the circuit model, whether it be a passive element or a controlled generator, can be found by choice of an appropriate injection point. In such a case, the purpose is to examine the sensitivity of H to variations of a selected component by finding a T and a T_n that are directly (or inversely) proportional to the value of that component. This can be done by injection either of a current j_z in parallel with, or a voltage e_z in series with, the selected component.

For example, in Fig. 8, the sensitivity of G to the transconductance $g_{m2}=1/r_{m2}$ of the second device can be found by injection of j_z or e_z at $W_4X_4Y_4$. For current injection the result is $T=Z_d/r_{m2}$, $T_n=Z_n/r_{m2}$ where Z_d and Z_n are the driving point impedances seen by r_{m2}, with e_i zero and with v_o nulled, respectively. The corresponding reference gain G^{i_y} is the closed-loop gain with $g_{m2}=\infty$, and the GFT reduces to the series form of the EET with r_{m2} identified as the extra element. For voltage injection, T and T_n are the reciprocals of the above expressions, and the GFT reduces to the parallel form of the EET.

It should be reiterated that the various sets of second-level transfer functions that result from different test signal injection conditions are not "wrong"; when inserted into the GFT they all lead to the same first-level result for G. The principal set that produces $G_\infty=1/K=(R_1+R_2)/R_1$ is preferred because of its direct interpretation in terms of the circuit properties, and is therefore the most useful for design purposes.

Throughout the treatment of the example circuit of Fig. 8, the source resistance R_s has been taken as zero, merely because this makes four of the eight third-level T's and T_n's infinite. A nonzero R_s makes the symbolic calculations more complicated, but a circuit simulator handles the numerical calculations just as easily. Results will be briefly mentioned for the preferred injection point at $W_2X_3Y_3$ in Fig. 8, as shown in Fig. 9 but with R_s=0.33k reinstated.

The four third-level transfer functions $T_i^{v_x}, T_v^{i_x}, T_{ni}^{v_x}, T_{nv}^{i_x}$ are no longer infinite, and allow the redundant definitions of T_{iv} and T_{niv} of (15) and (16) to be confirmed. Nevertheless, these two quantities remain negligibly large in (66) and (67). Also, $T_v^{i_y}$ remains negligibly large, and $T \approx T_i^{v_y}$ is the same up to about 300MHz, so the real loop gain crossover frequency remains at 32MHz.

Although G_∞=20dB is the same for R_s=0.33k as for R_s=0, there is a considerable difference in the closed-loop gain G. In Fig. 10, the apparent peaked response of G drops below 20dB at 1GHz, but with R_s=0.33k this occurs at 70MHz, more than a decade lower. Moreover, G is asymptotic at infinite frequency to a much lower value. This can be seen directly from Fig. 8, with C_1 and C_2 short at infinite frequency: v_o/e_i is approximately $r_{m2}/(r_{m2}+R_s)$, which is -23dB compared to 0dB for R_s=0 as in Fig. 10.

If it seems surprising that only a 0.33k source resistance causes more than a decade loss of bandwidth in an amplifier that implements input voltage differencing which raises an already high input impedance, it must be remembered that the feedback multiplication factor drops to unity beyond loop gain crossover, and that the open-loop input impedance is mainly capacitive anyway. The input admittance Y_i could be investigated in detail by application of the GFT with H replaced by Y_i, but this will not be pursued here.

6. Conclusions

The GNT expresses a "first level" transfer function H of a linear circuit model in terms of four "second level" transfer functions H_∞, T, T_n, and H_0. There is a redundancy relation (45), $H_0 / H_\infty = T / T_n$, between the four second level transfer functions, so that the GNT can be expressed in terms of any three. Of the four versions, two are given in (59) and (60), repeated below:

$$H = H_\infty \frac{1+\frac{1}{T_n}}{1+\frac{1}{T}} \qquad (140) \qquad\qquad H = H_\infty \frac{T}{1+T} + H_0 \frac{1}{1+T} \qquad (141)$$

The format of the GNT can be represented by the "natural" block diagram of Fig. 7. The GNT is derived in Section 2 as an application of the EET in which T is identified as the total return ratio of a fictitious ideal transformer inserted into the circuit model.

The second level transfer functions can be calculated in terms of one or more third level transfer functions, each of which is calculated under certain conditions imposed upon one or more test signals injected into the linear circuit model of the system in place of the fictitious ideal transformer, as in Fig. 6. A test signal can be a current or a voltage (single injection), or current and voltage injected at the same point (dual injection); variations and extensions are possible, but are not discussed

in this paper. The nodes WXY in Fig. 6 identify a dual, a current, or a voltage injection point.

For dual test signal injection, T and T_n are each a "triple parallel combination", according to (20) and (21), of three third level transfer functions given by (22) through (29) and (15), (16). By (19) H_∞ is directly equal to the third level $H^{i_y v_y}$ given by (9), and by (49), H_0 is the weighted sum of three third level transfer functions given by (50) through (52).

For single test signal injection, each of the four second level transfer functions is directly equal to a third level transfer function, given by (38) through (40) and (55) for current injection, and by (41) through (43) and (58) for voltage injection.

Different injection points produce different sets of second level transfer functions H_∞, T, T_n, and H_0. although each set when inserted into the GNT leads to the same first level transfer function H, and all sets fit the block diagram of Fig. 7

Since the "natural" block diagram of Fig. 7 is the same as that of the augmented single loop feedback system of Fig. 3 or 4, it is equally natural to re-name the GNT as the General Feedback Theorem, the GFT, and to interpret the various transfer functions in terms of familiar feedback nomenclature. This is done in Section 3, in which T is identified as the loop gain, T_n is the null loop gain, and H_∞ and H_0 are respectively the first level transfer function with infinite loop gain and with zero loop gain. If H represents a "gain" G, alternative interpretations are that G_∞ is the "ideal closed-loop gain", and G_0 is the "direct forward transmission" which includes feedforward through any minor loop feedback path as well as feedforward through the major loop feedback path.

The fact that Fig. 7 and Fig. 3 or 4 are the same is the link between general feedback theory and analysis based on an empirical, or "guessed," block diagram. A designer/analyst typically has constructed a tentative circuit that embodies the block diagram of Fig. 4 and has made the K block equal to the reciprocal of the desired closed-loop gain, which is Design Step #1 of Section 1. If a GFT injection point is chosen inside the major loop but outside any minor loops, and also so that $G_\infty = 1/K$, the corresponding set of second level transfer functions constitutes the "principal set" in which T is the principal loop gain, and Design Steps #2 through #4 can then be accomplished.

The GFT is illustrated in Section 4 by application to the two-stage feedback amplifier of Fig. 8. In Section 4.1, the first level transfer function H is identified as the closed-loop voltage gain G, and the principal set of second level transfer functions G_∞, T, T_n, G_0 is established by choice of the injection point $W_2X_3Y_3$ in Fig. 9. For dual test signal injection, all the third level transfer functions are null injection calculations, which are accomplished by the "short cut" method of following the transfer function input signal to its output signal, incorporating the nulled signals en route. This method leads to low entropy expressions in which suitable approximations can easily be recognized, and which can easily be put into factored pole-zero form.

Some practice is needed for one to become convinced that null injection calculations are actually simpler and easier than conventional single injection calculations, and so the analysis is described in considerable detail. In addition, for further insight into null injection, the 2EET is employed to arrive at some of the

third-level transfer functions that are themselves defined under null injection conditions.

All transfer functions can be calculated numerically with use of a circuit simulator, and most of the results for the circuit of Fig. 8 are displayed in the graphs of Section 4. All confirm the symbolic results, including the closed-loop gain G given alternatively by (61) in Fig. 13 or (62) in Fig. 16, both of which are identical to the result by direct simulation.

To illustrate that the GFT applies to any transfer function of a linear system model, in Section 4.2 H is identified as Z_o, the output impedance of the feedback amplifier of Fig. 8, and again all the symbolic results are confirmed in Fig. 17 by the circuit simulator.

Although any circuit simulator can be programmed to do null injection calculations, Intusoft's ICAP/4 contains a special GFT subprogram in which all the necessary calculations are preconstructed, so that a designer/analyst unfamiliar with null injection can easily and quickly obtain all the desired graphical results.

Section 5 includes a discussion of how the results for the feedback amplifier of Fig. 8 are changed if different test signal injection points are chosen. Different sets of second level transfer functions G_∞, T, T_n, G_0 all produce the same first level transfer function G, but may not have G_∞ equal to $1/K$, the reciprocal of the feedback divider ratio, and so may be less useful for design purposes. However, an injection point chosen at a selected circuit element can produce a T and a T_n that represent return ratios for that element, and so are useful for sensitivity calculations. In this form the GFT reduces to the single Extra Element Theorem — from whence it came.

References

1. Wai-Kai Chen, *The Circuits and Filters Handbook*, CRC Press, 1995; Section V by John Choma Jr. and Wai-Kai Chen

2. Paul R. Gray, Paul J. Hurst, Stephen H. Lewis, and Robert G. Meyer, *Analysis and Design of Analog Integrated Circuits*, John Wiley & Sons, Inc. New York, 4th Edition, 2001; Chapter 8.

3. R.D.Middlebrook, "Design-Oriented Analysis of Feedback Amplifiers," *Proc. National Electronics Conf.,* vol. XX, pp. 234-238, Oct. 1964.

4. R.D.Middlebrook, "Measurement of Loop Gain in Feedback Systems," *Int. J. Electronics,* vol. 38, no. 4, pp. 485-512, 1975.

5. John Lindal and R. David Middlebrook, "Design-Oriented Analysis: Supplementary Notes for EE14 and EE114," EE Dept., California Institute of Technology, 1995.

6. R.D.Middlebrook, "Null Double Injection and the Extra Element Theorem," *IEEE Trans. on Education,* vol. 32, no. 3, pp. 167-180, Aug. 1989.

7. R.D.Middlebrook, "The Two Extra Element Theorem," *Proc. IEEE Frontiers in Education,* Twenty-First Annual Conf., Purdue Univ., pp. 702-708, Sept. 21-24, 1991.

8. R.D.Middlebrook and Vatché Vorpérian, "The *N* Extra Element Theorem," *IEEE Trans. on Circuits and Systems—I: Fundamental Theory and Applications,* vol. 45, no. 9, pp. 919-935, Sept. 1998.

9. Vatché Vorpérian, *Fast Analytical Techniques in Electrical and Electronic Circuits.* London, UK: Cambridge Univ. Press, 2002.

10. R.D.Middlebrook, "Low-Entropy Expressions: the Key to Design-Oriented Analysis," *Proc. IEEE Frontiers in Education,* Twenty-First Annual Conf., Purdue Univ., pp. 399-403, Sept. 21-24, 1991.

11. Michael Hassul, "BJT-FET Comparison: A New FET Model," *IEEE Trans. on Education,* vol. 39, no. 1, pp. 92-94, Feb. 1996.

12. R.D.Middlebrook, "Methods of Design-Oriented Analysis: The Quadratic Equation Revisited," *Proc. IEEE Frontiers in Education,* Twenty-Second Annual Conf., Vanderbilt Univ., pp. 95-102, Nov. 11-15, 1992.

13. Paul J. Hurst, "A Comparison of Two Approaches to Feedback Circuit Analysis," IEEE *Trans. on Education,* vol. 35, no. 3, pp. 253-261, Aug. 1992.

Figure Captions

Fig. 1. The basic single-loop feedback block diagram.

Fig. 2. Injection of a test signal u_z for determination of the ideal closed-loop gain G_∞ and the loop gain T.

Fig. 3. Augmented diagram that incorporates a G_0 block to represent direct forward transmission.

Fig. 4. Recognition of minor loops (bidirectional transmission) inside the major feedback loop.

Fig. 5. (a) Generalized linear network model with identification of arbitrary nodes W and XY.

(b) Insertion of an ideal transformer at W, X, and Y. When A_i =1 and A_v = 1, the transformer is transparent and does not affect the system properties.

Fig. 6. Injection of dual test signals i_z and v_z in place of the ideal transformer for determination of the third-level null double injection and double null triple injection quantities needed to obtain the second-level transfer functions that constitute the general network theorem of (18) or (44).

Fig. 7. "Natural" block diagram model that represents the GFT, whose format is identical to that of Fig. 3 or 4. The individual blocks are described in terms of three out of four of a set of second level transfer functions that are calculated unambiguously from the detailed circuit diagram, rather than being guessed *a priori*.

Fig. 8. Example of a small-signal linear model of a two-stage feedback amplifier, showing some possible test signal injection points WXY. Resistances are in $\mathrm{k}\Omega$, capacitances in pF. All the following figures through Fig. 17 are for the circuit of Fig. 8 with $\alpha_1, \alpha_2 = 1$, $R_s = 0$.

Fig. 9. Selection of dual current and voltage injection point $\mathrm{W_2X_3Y_3}$ that establishes the principal set of second level transfer functions G_∞, T, T_n, G_0 in which G_∞ is made equal to the reciprocal feedback ratio $1/K = (R_1 + R_2)/R_1$. This is a "template" model upon which appropriate sets of signal conditions can be imposed for calculation of the various third-level transfer functions.

Fig. 10. Components G_∞, T, and T_n of the closed-loop gain $G = v_o/e_i$. The result calculated by the GFT is indistinguishable from that by direct simulation. Transfer functions in this and the following figures are magnitudes unless otherwise indicated.

Fig. 11. Another "template" model of the circuit of Fig. 9 for calculation of $M = i/i_x$ upon which appropriate sets of signal conditions can be imposed for reinstatement of the two impedances Z_1 and Z_2 by the 2EET.

Fig. 12. (a) The components $T_i^{v_y}$ and $T_v^{i_y}$ of T; T_{iv} is infinite. The principal loop gain T is dominated by $T_i^{v_y}$ at all frequencies, so the phase of T is essentially the same as the phase of $T_i^{v_y}$.

(b) The components $T_{ni}^{v_y}$ and $T_{nv}^{i_y}$ of T_n ; T_{niv} is infinite. The principal null loop gain T_n is dominated by $T_{ni}^{v_y}$ at all frequencies.

Fig. 13. Closed-loop gain G dissected according to (61) into the product of $G_\infty D$ and the null discrepancy factor D_n. Above the T_n crossover frequency f_{nc}=17MHz, D_n increases above unity, and G increases above $G_\infty D$.

Fig. 14. Response of the output voltage $v_o(t)$ to a step in e_i of 1V. There is a huge undershoot resulting from the 360° phase change of G from zero to infinite frequency.

Fig. 15. Direct forward transmission G_0 and its weighting factor $(1-D)$.

Fig. 16. Closed-loop gain G dissected according to (62) into the sum of the weighted ideal closed loop gain $G_\infty D$ and the weighted direct forward transmission $G_0(1-D)$. Above the T_n crossover frequency f_{nc}=17MHz, the second term overtakes the first and G increases above $G_\infty D$, as in Fig. 13.

Fig. 17. The components Z_{o0} and $(1-D)$ of the output impedance Z_o ; $Z_{o\infty}$ is zero. The result $Z_o = Z_{o0}(1-D)$ of (129) calculated by the GFT is indistinguishable from that by direct simulation.

Fig. 18. Absorption of the direct forward transmission block G_0 of Fig. 7 into a pseudo forward gain block $H_\infty T_p$ in terms of a pseudo loop gain T_p.

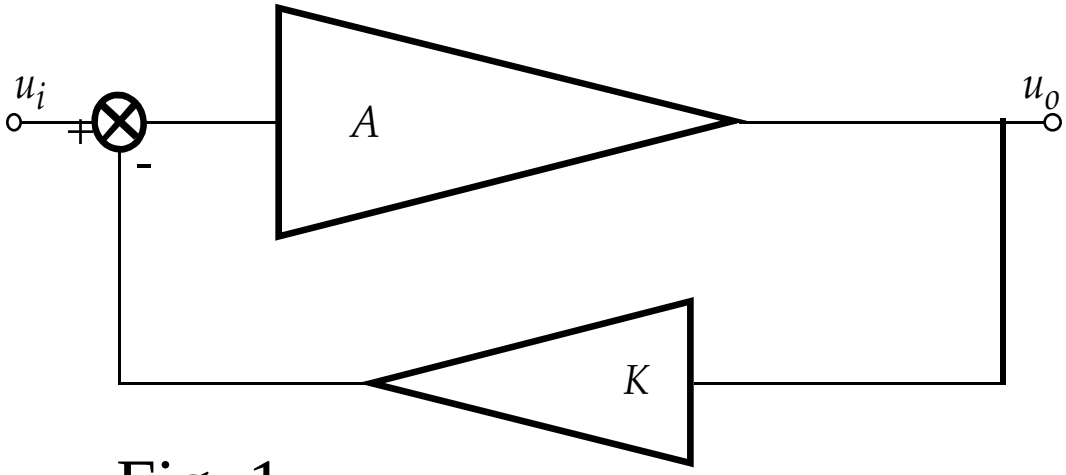

Fig. 1

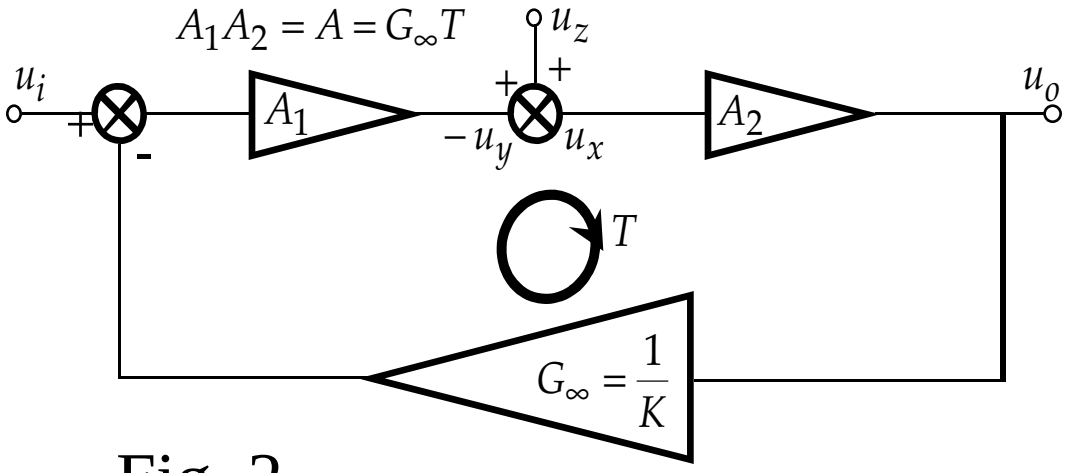

Fig. 2

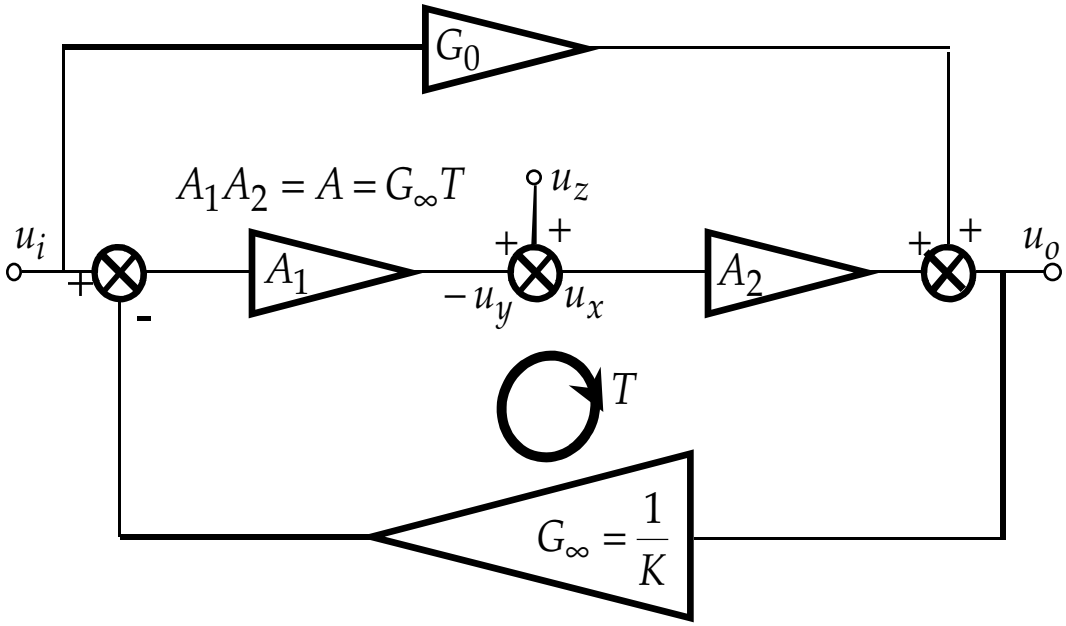
G_0
$A_1 A_2 = A = G_\infty T$
u_z
u_i
A_1
A_2
u_o
$-u_y$
u_x
T
$G_\infty = \frac{1}{K}$

Fig. 3

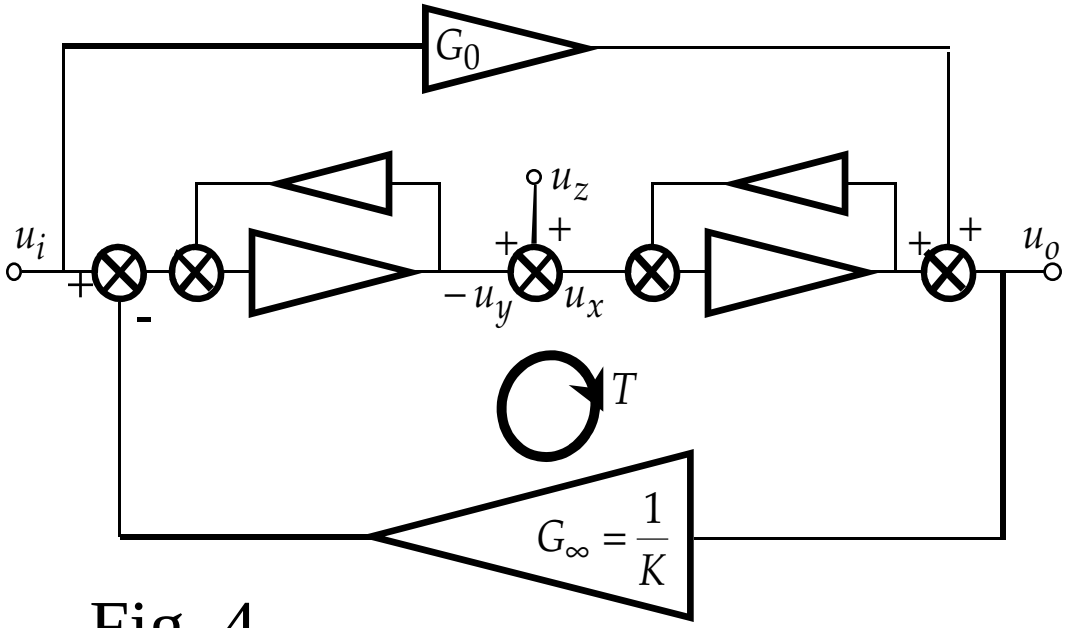
G_0
u_z
u_i
u_o
$-u_y$
u_x
T
$G_\infty = \frac{1}{K}$

Fig. 4

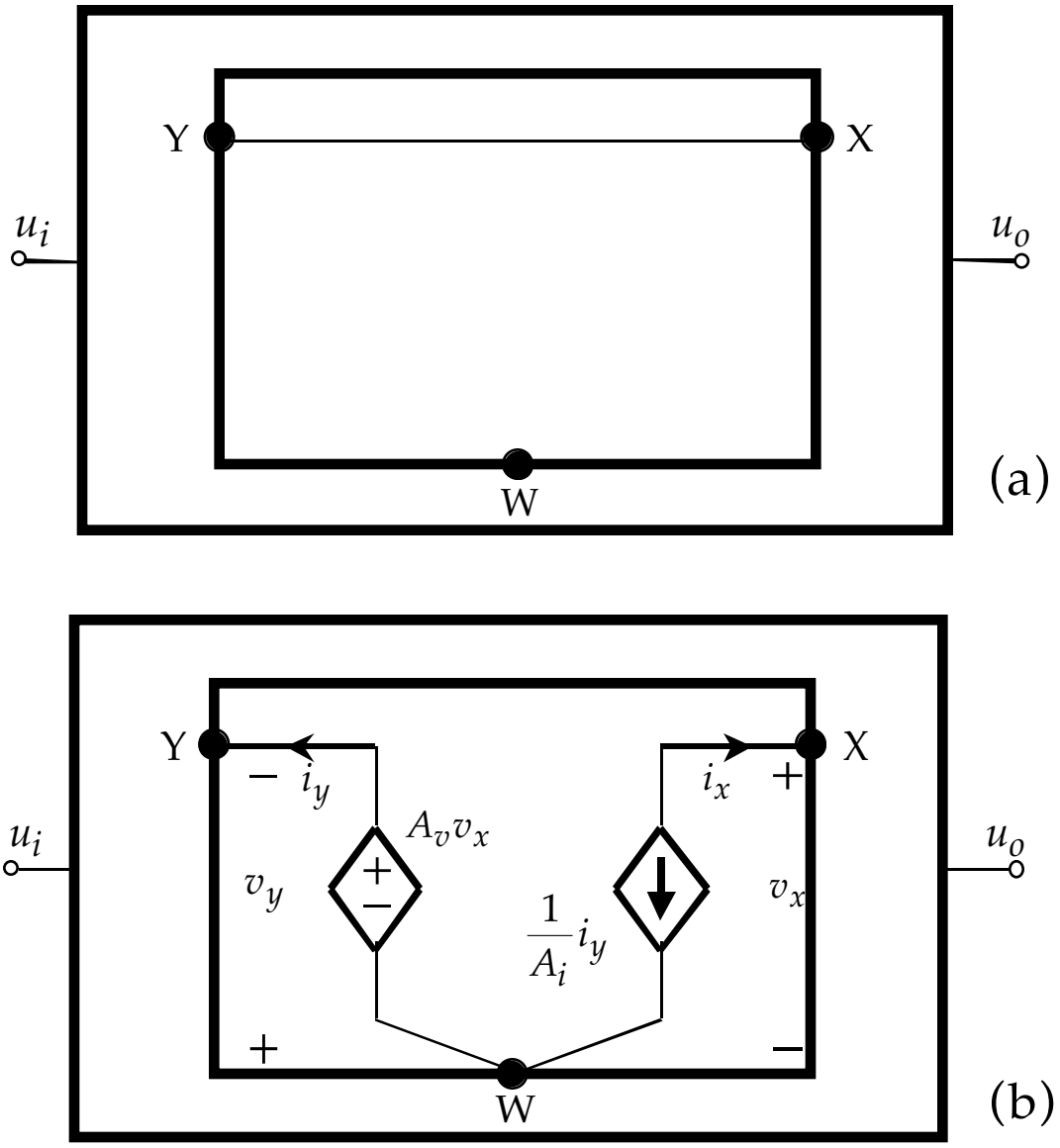

Fig. 5

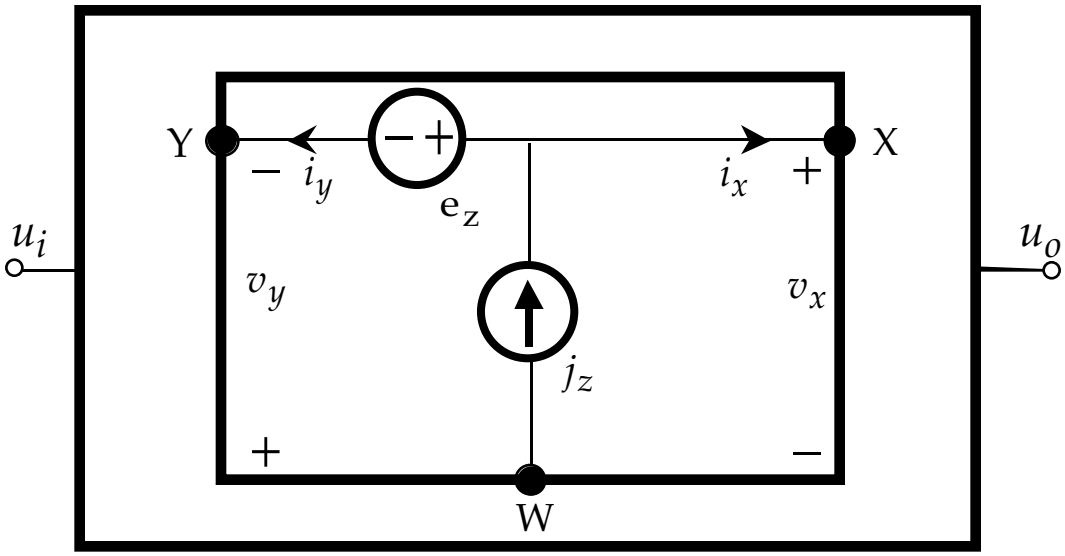
Y
X
W
u_i
u_o
i_y
i_x
e_z
v_y
v_x
j_z
+
−

Fig. 6

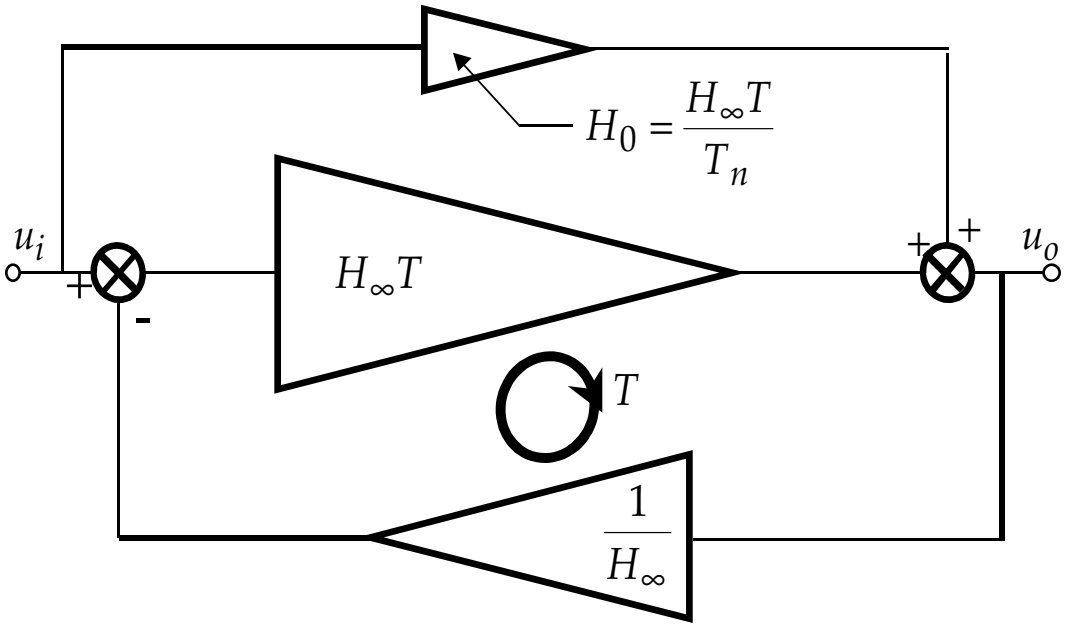
$H_0 = \frac{H_\infty T}{T_n}$
u_i
u_o
$H_\infty T$
T
$\frac{1}{H_\infty}$
+
-

Fig. 7

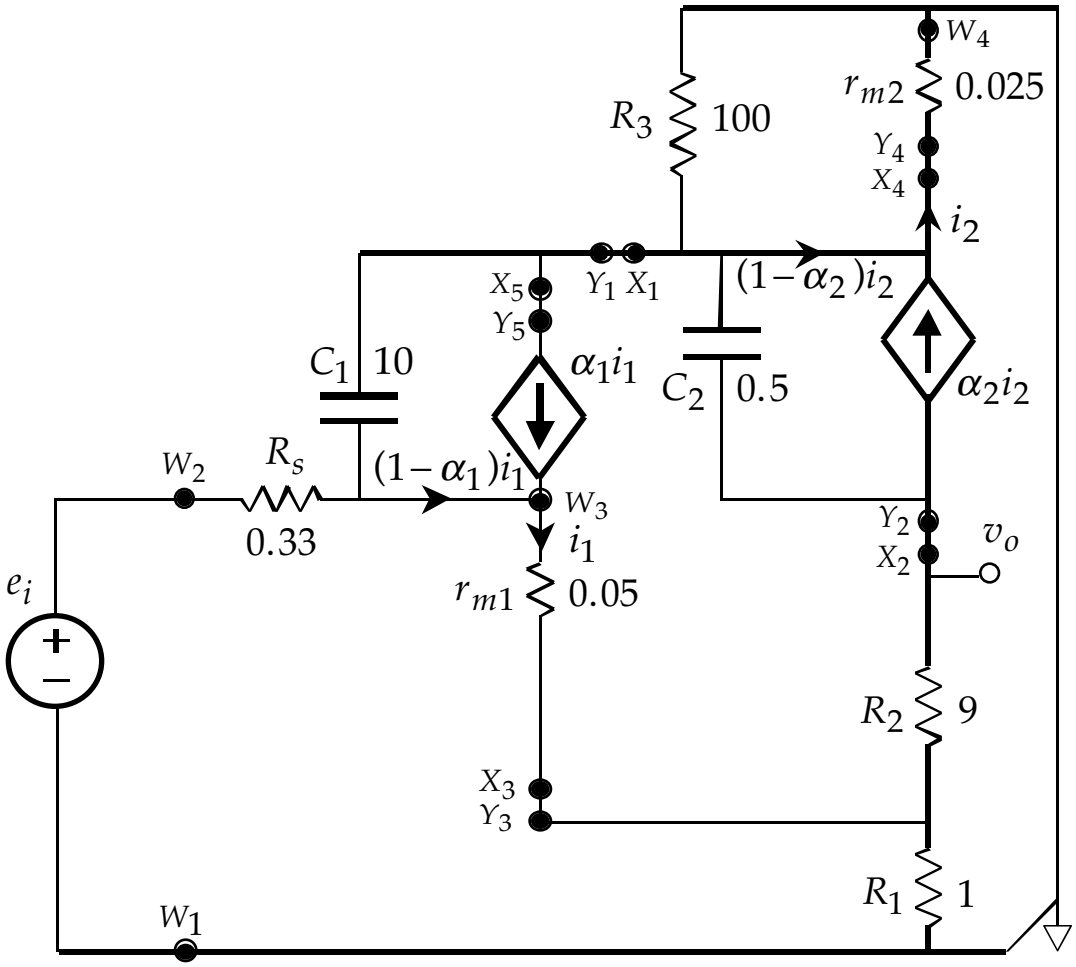
W_4
r_{m2} 0.025
R_3 100
Y_4
X_4
i_2
X_5
Y_5
Y_1 X_1
$(1-\alpha_2)i_2$
C_1 10
$\alpha_1 i_1$
C_2 0.5
$\alpha_2 i_2$
W_2
R_s
0.33
$(1-\alpha_1)i_1$
W_3
i_1
Y_2
X_2
v_o
e_i
r_{m1} 0.05
R_2 9
X_3
Y_3
R_1 1
W_1

Fig. 8

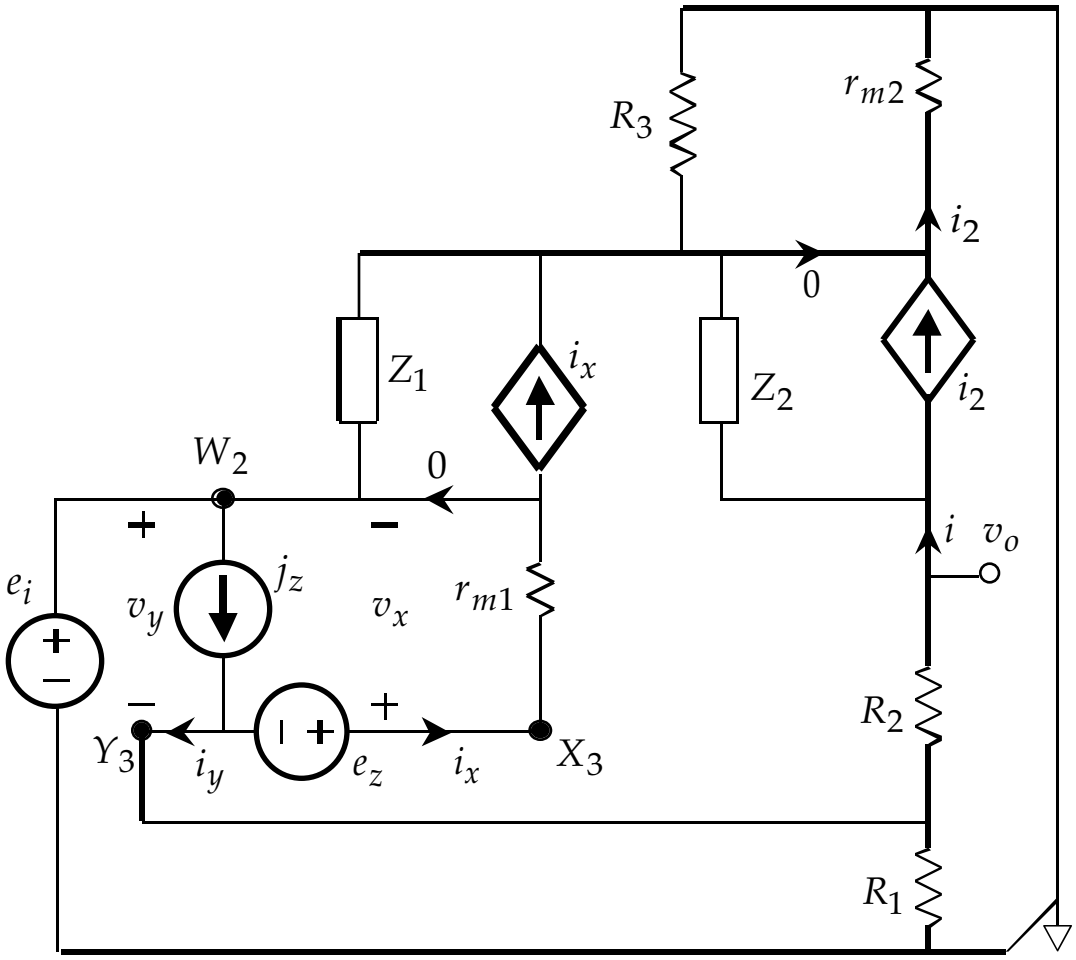

Fig. 9

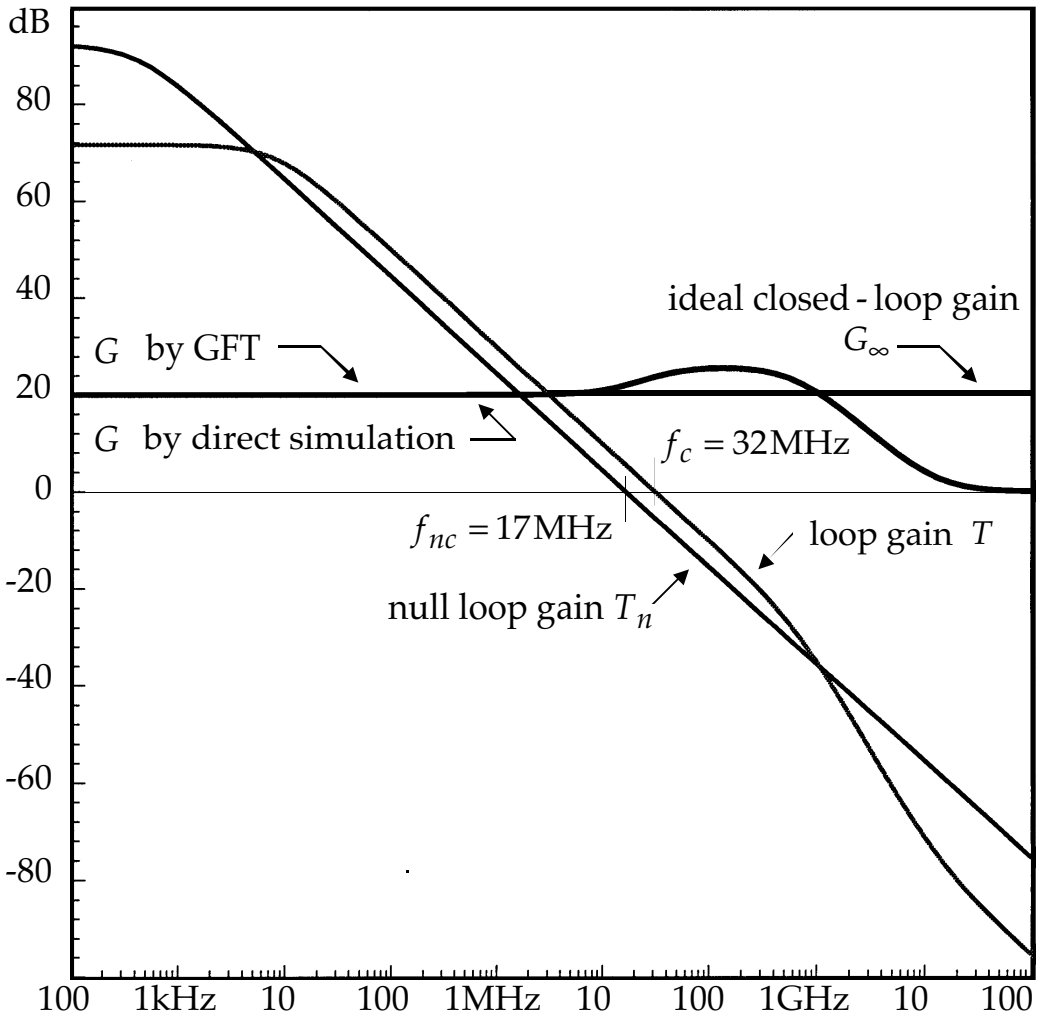
dB
80
60
40
20
0
-20
-40
-60
-80
100
1kHz
10
100
1MHz
10
100
1GHz
10
100
ideal closed - loop gain
G_∞
G by GFT
G by direct simulation
$f_c = 32\text{MHz}$
$f_{nc} = 17\text{MHz}$
loop gain T
null loop gain T_n

Fig. 10

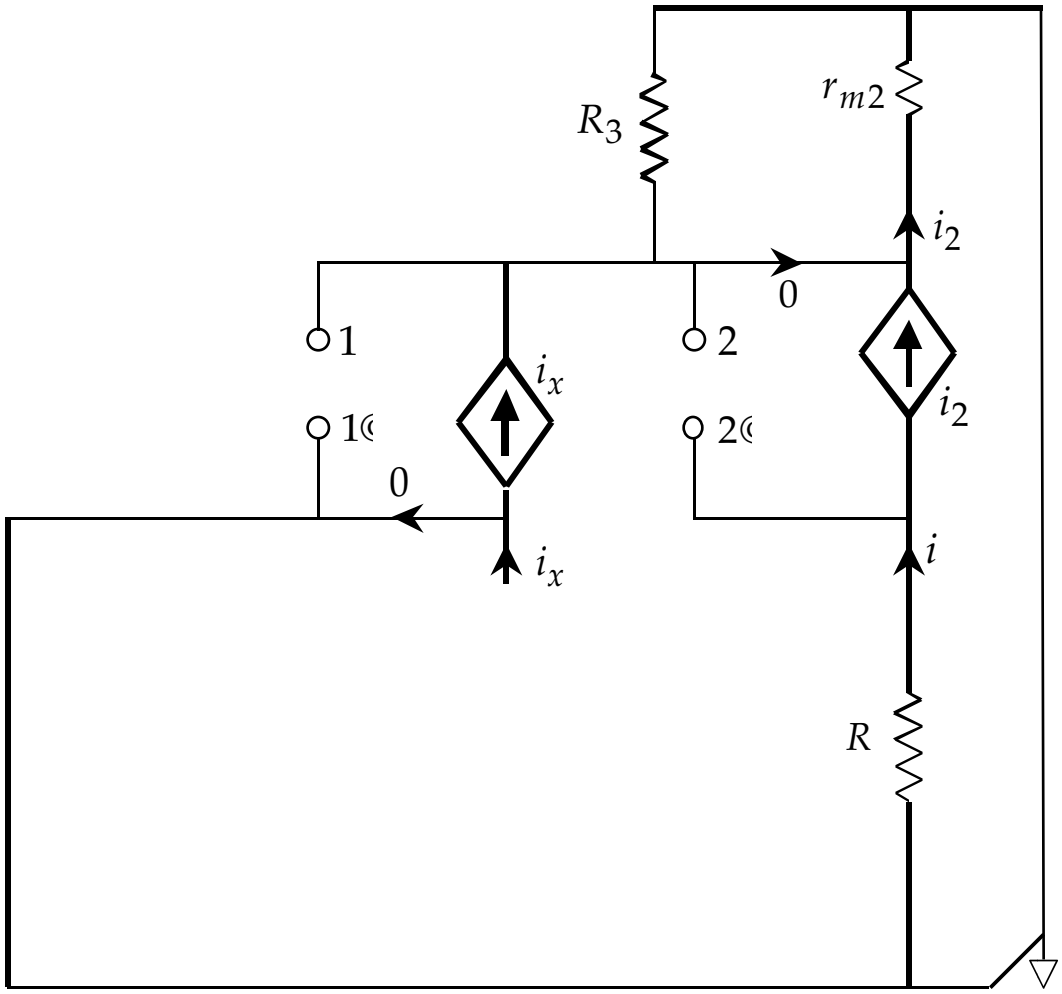

Fig. 11

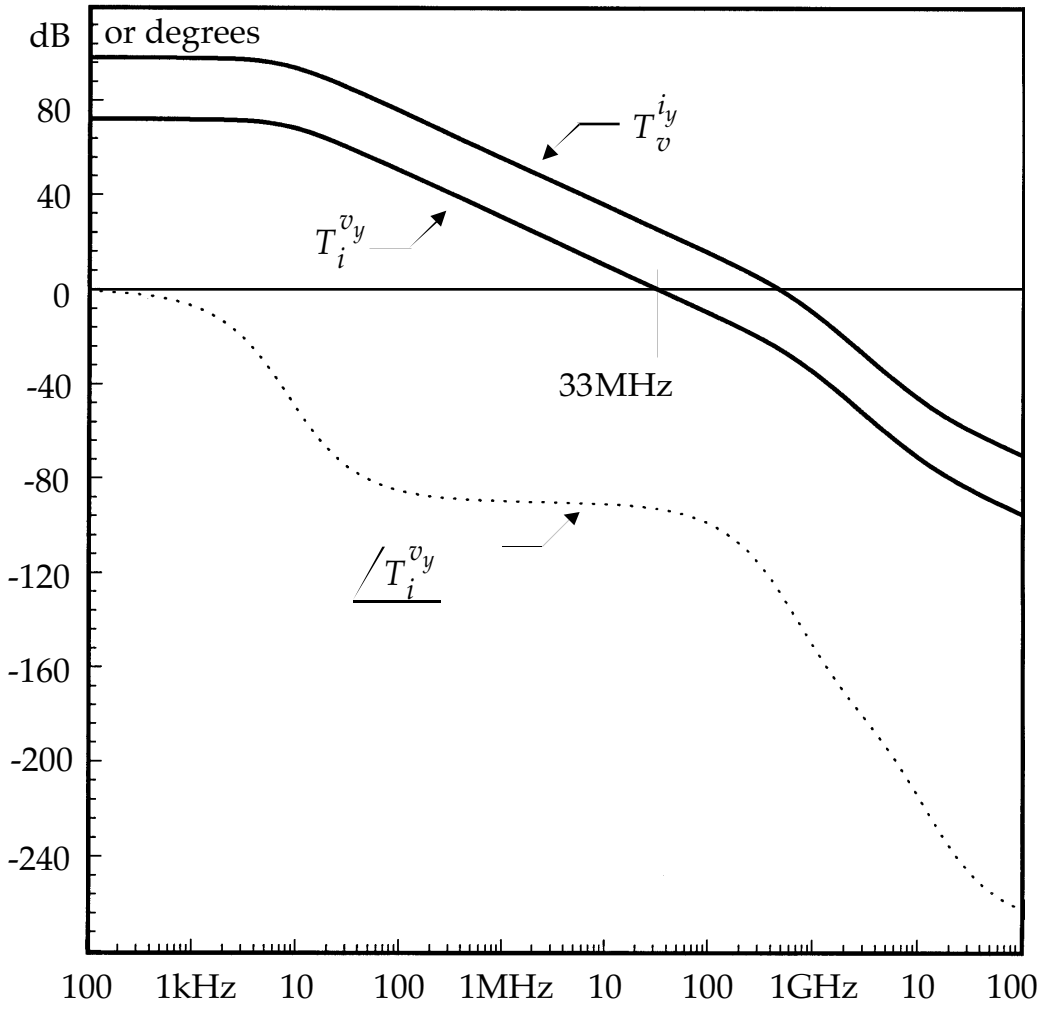
dB
or degrees
80
40
0
-40
-80
-120
-160
-200
-240
$T_v^{i_y}$
$T_i^{v_y}$
33MHz
$\angle T_i^{v_y}$
100
1kHz
10
100
1MHz
10
100
1GHz
10
100

Fig. 12(a)

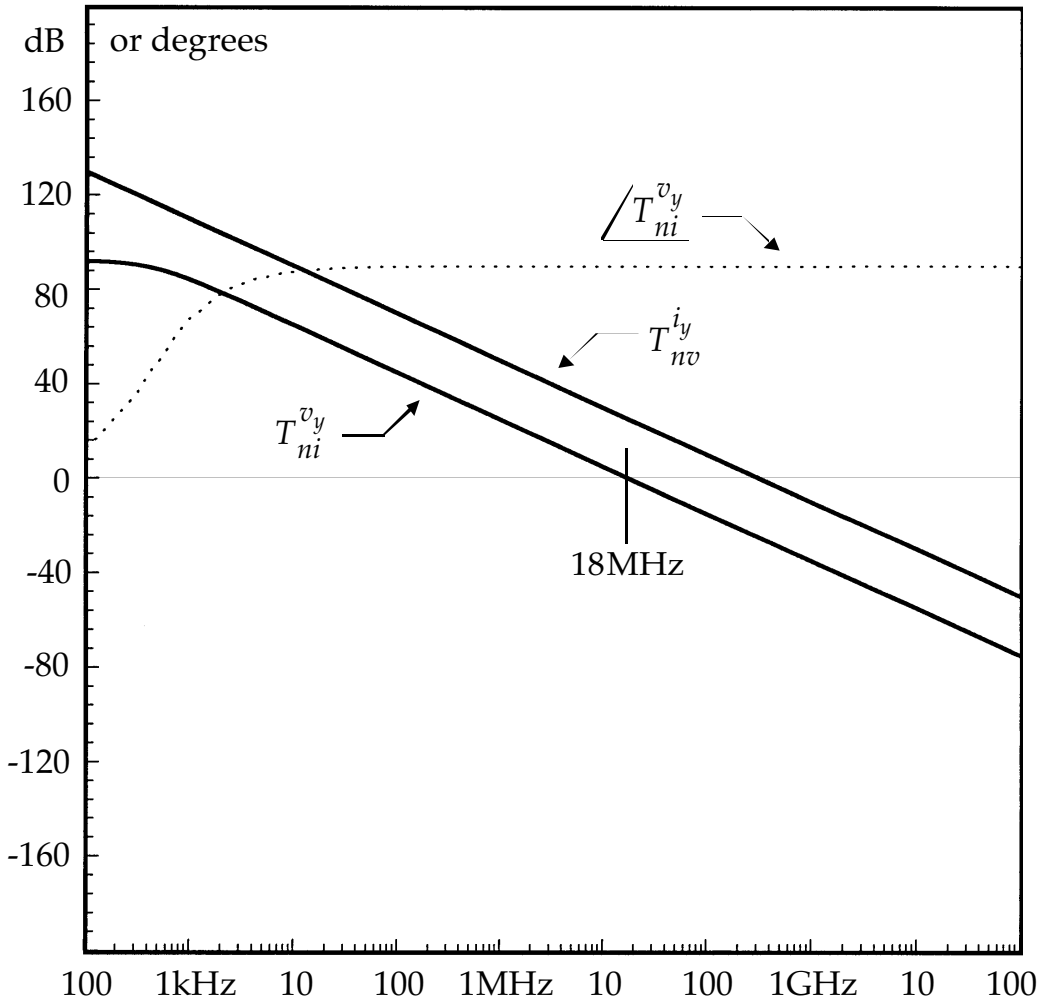
dB
or degrees
160
120
80
40
0
-40
-80
-120
-160
$\angle T_{ni}^{v_y}$
$T_{nv}^{i_y}$
$T_{ni}^{v_y}$
18MHz
100
1kHz
10
100
1MHz
10
100
1GHz
10
100

Fig. 12(b)

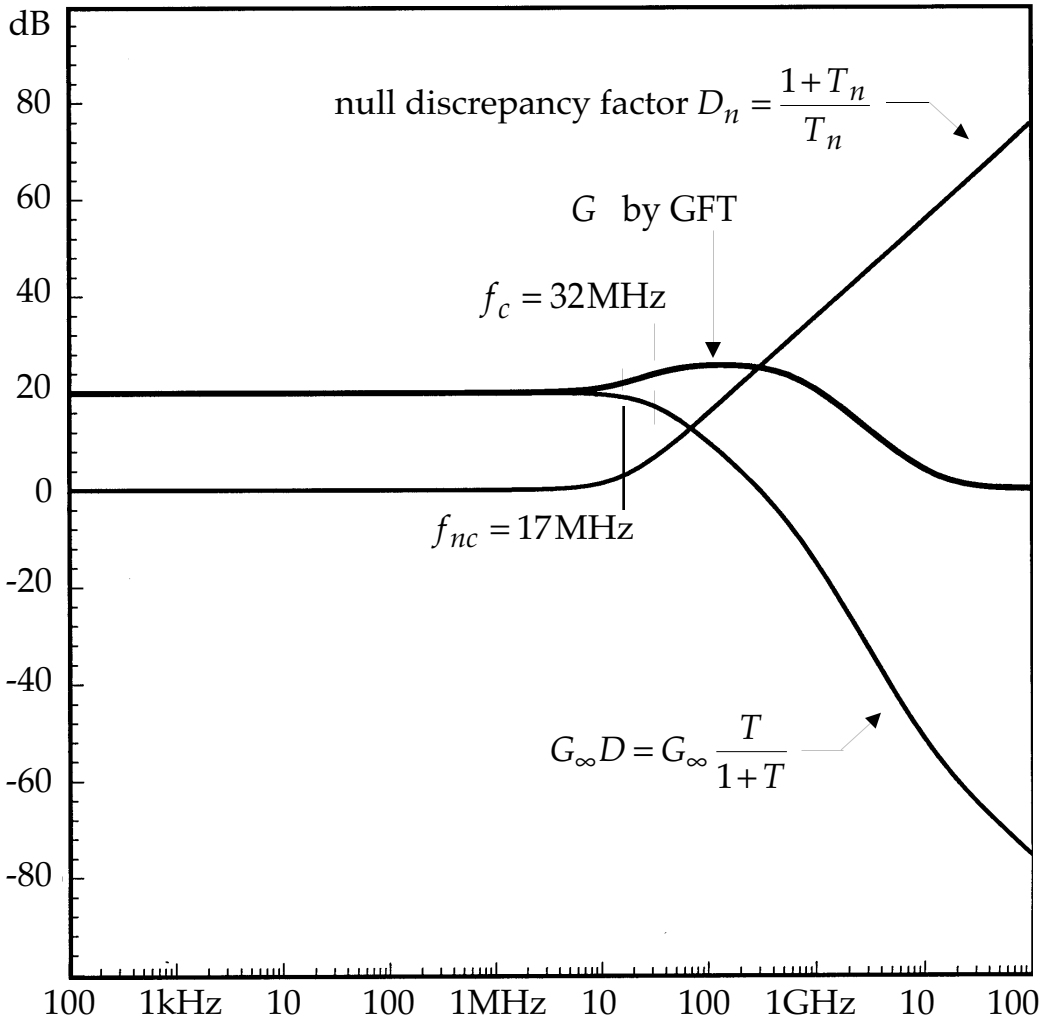
dB
80
60
40
20
0
-20
-40
-60
-80
null discrepancy factor $D_n = \frac{1+T_n}{T_n}$
G by GFT
$f_c = 32\text{MHz}$
$f_{nc} = 17\text{MHz}$
$G_\infty D = G_\infty \frac{T}{1+T}$
100
1kHz
10
100
1MHz
10
100
1GHz
10
100

Fig. 13

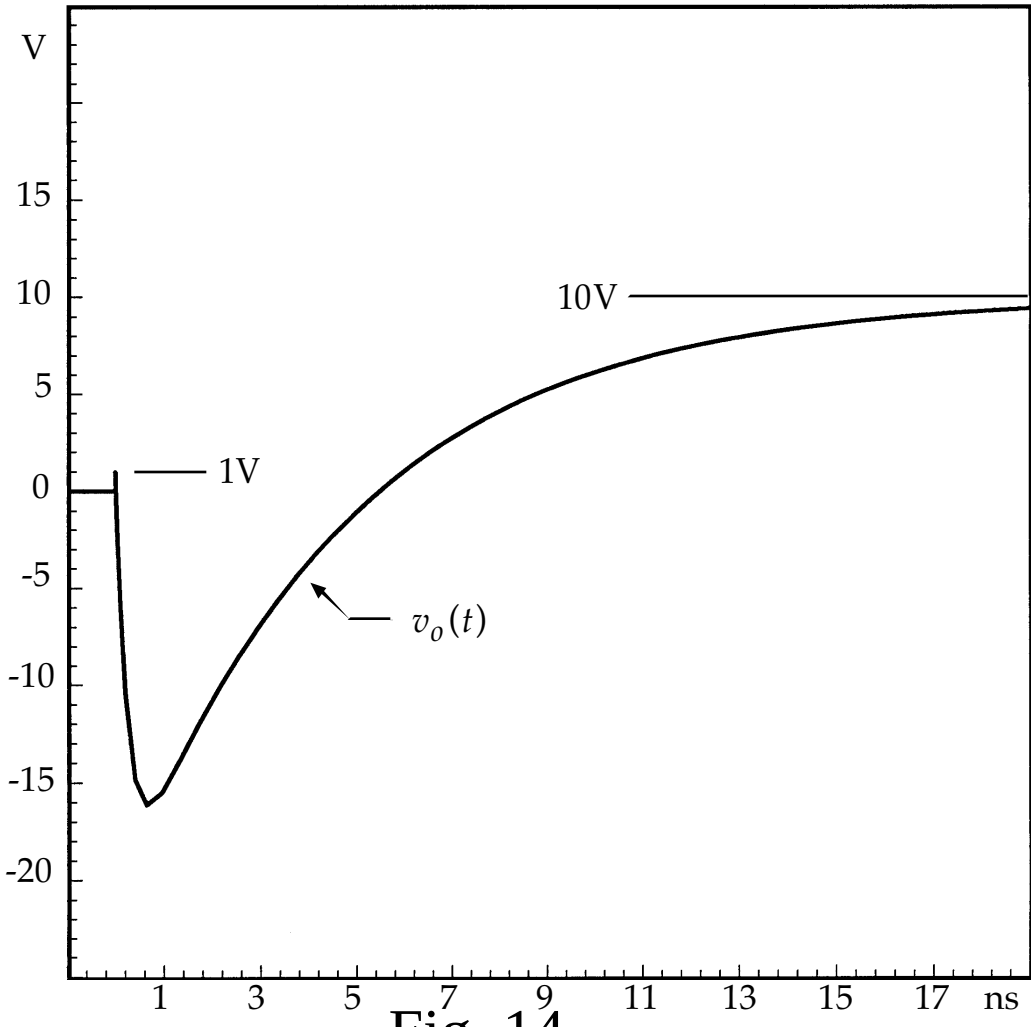

Fig. 14

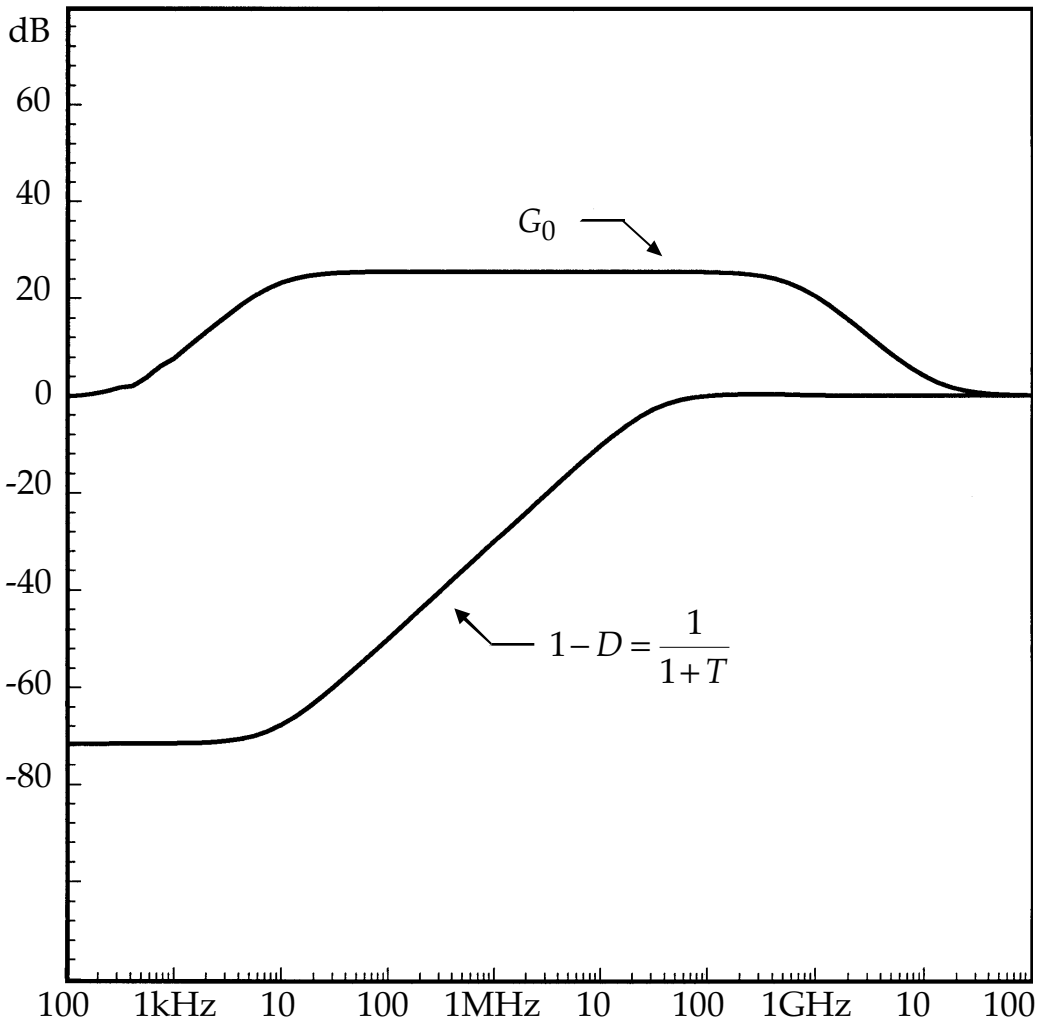
dB
60
40
20
0
-20
-40
-60
-80
G_0
$1-D=\frac{1}{1+T}$
100
1kHz
10
100
1MHz
10
100
1GHz
10
100

Fig. 15

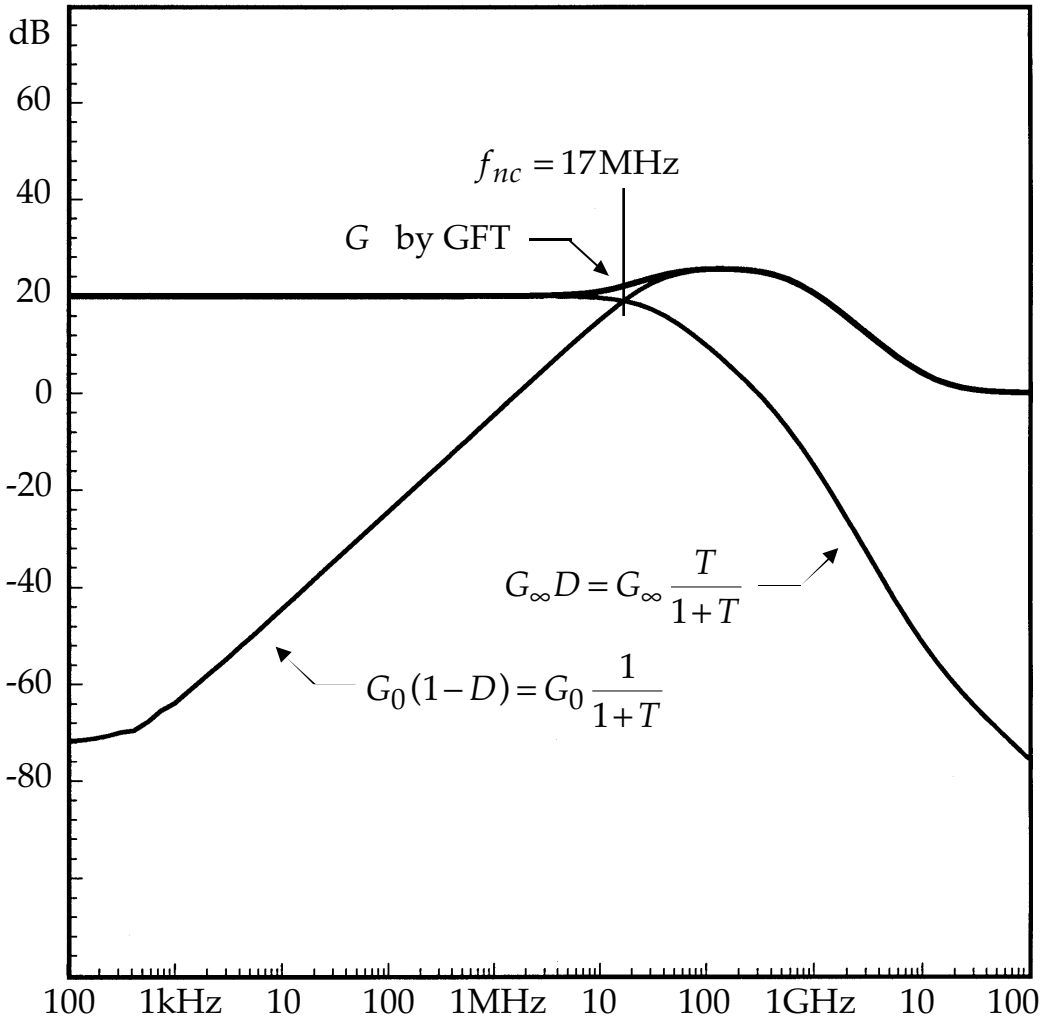
dB
60
40
20
0
-20
-40
-60
-80
$f_{nc} = 17\text{MHz}$
G by GFT
$G_\infty D = G_\infty \frac{T}{1+T}$
$G_0(1-D) = G_0 \frac{1}{1+T}$
100
1kHz
10
100
1MHz
10
100
1GHz
10
100

Fig. 16

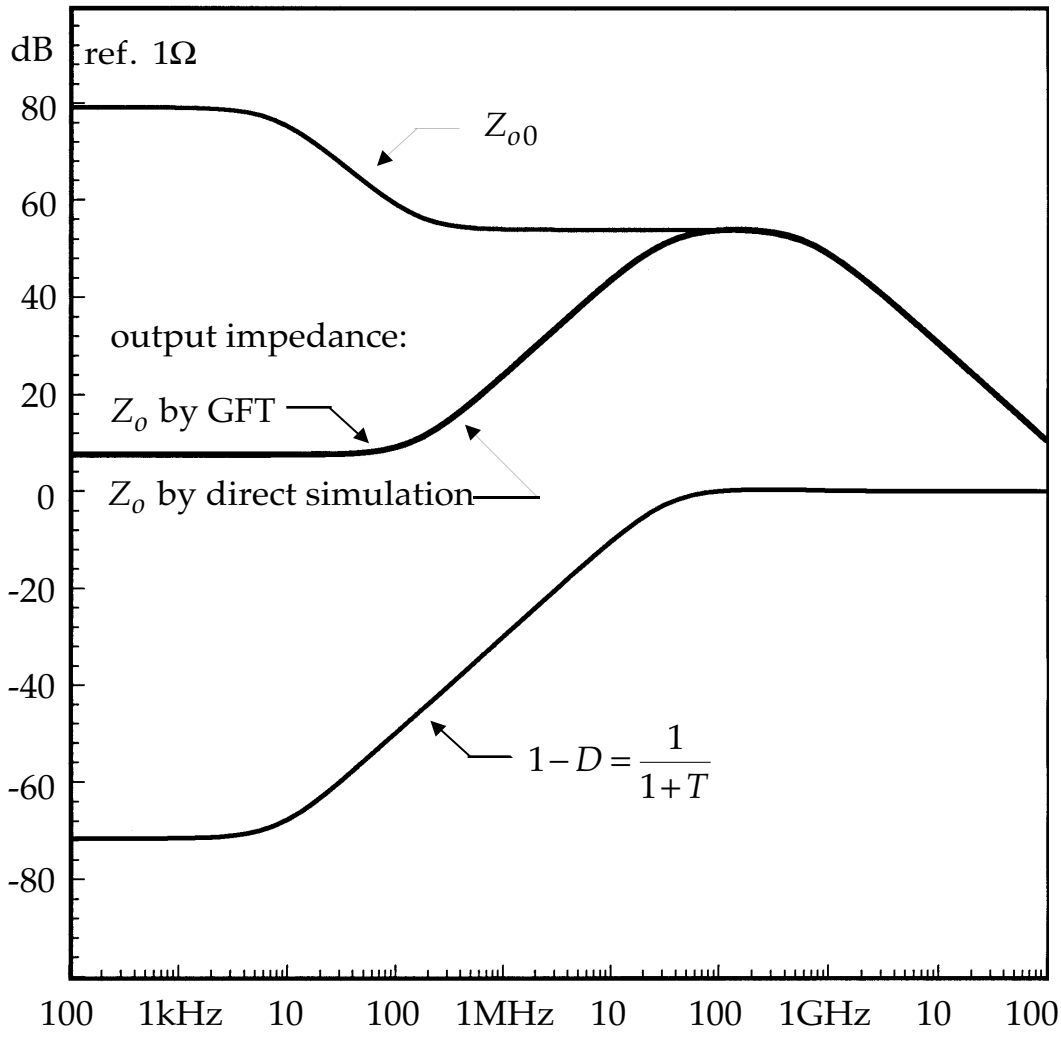
dB
ref. 1Ω
80
60
40
20
0
-20
-40
-60
-80
Z_{o0}
output impedance:
Z_o by GFT
Z_o by direct simulation
$1-D=\frac{1}{1+T}$
100
1kHz
10
100
1MHz
10
100
1GHz
10
100

Fig. 17

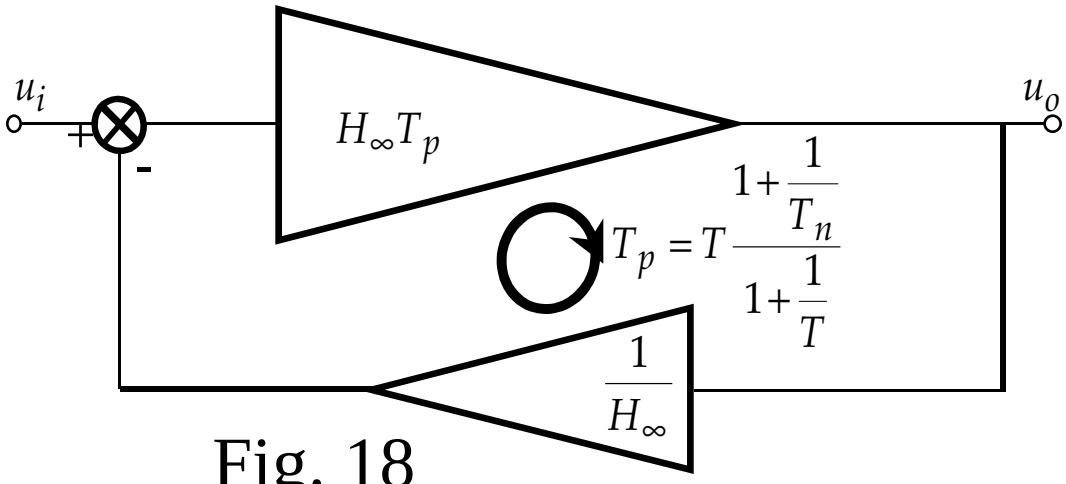

Fig. 18